POLITÉCNICO DE LEIRIA
ESCOLA SUPERIOR DE TECNOLOGIA E GESTÃO

Polytechnic of Leiria
School of Technology and Management
Department of Electrical and Electronics Engineering
Master in Electrical and Electronic Engineering – Electronics and Telecommunications

DISSERTATION

ELECTRONICALLY RECONFIGURABLE FSS-INSPIRED TRANSMITARRAY FOR TWO DIMENSIONAL BEAMSTEERING FOR 5G AND RADAR APPLICATIONS AT 28 GHZ

MÁRIO ANTÓNIO PATRÍCIO CARREIRA VALA

Leiria, September of 2019

This page is intentionally left blank.

Polytechnic of Leiria
School of Technology and Management
Department of Electrical and Electronics Engineering
Master in Electrical and Electronic Engineering – Electronics and Telecommunications

DISSERTATION

ELECTRONICALLY RECONFIGURABLE FSS-INSPIRED TRANSMITARRAY FOR TWO DIMENSIONAL BEAMSTEERING FOR 5G AND RADAR APPLICATIONS AT 28 GHZ

MÁRIO ANTÓNIO PATRÍCIO CARREIRA VALA
Number: 2172276

Dissertation supervised by Professor Rafael F. S. Caldeirinha (rafael.caldeirinha@ipleiria.pt) and Doctor João R. Reis (joao.reis@ipleiria.pt).

Leiria, September of 2019

This page is intentionally left blank.

ACKNOWLEDGMENTS

I would first like to thank my supervisors, Professor Rafael Caldeirinha and Doctor João Reis for the continuous guidance and assistance throughout this work, that allowed me to fulfill the objectives and achievements defined for this dissertation.

I would also like to thank the School of Technology and Management of Polytechnic of Leiria and the Instituto de Telecomunicações - Leiria (IT-Leiria), for granting me access to the laboratory facilities and radio equipment necessary for the completeness of this dissertation and, in particular, to project *RETIOT (SAICT-45-2015-03 / Projeto nº 16432)* for funding my research developments. I would also like to thank IT-Aveiro, particularly Professors João Nuno Matos and Pedro Cabral for allowing me to use some of their equipment and for helping me with some of the measurements needed to validate the developed prototype.

I would like to acknowledge my colleagues at IT-Leiria Antennas and Propagation group, especially André Sardo and Wilson Conniott for their support and willingness to help me when I most needed.

In addition, I would like to thank my parents and sister for their continuous support and for encouraging me to always continue forward and never give up. Lastly, a big thank you to my girlfriend for always staying by my side and supporting me even when things didn't go as planned.

This page is intentionally left blank.

ABSTRACT

In this dissertation, the author's work on a 28 GHz transmitarray capable of antenna beamsteering for various wireless applications, is presented. Such device allows for the adjustment of the radiation pattern of an antenna by changing its main lobe direction, without the need of any mechanical means.

A unit-cell based on a square-slot Frequency Selective Surface (FSS) is designed, simulated and optimised through several full-wave simulations, using an electromagnetic solver (CST MWS). Subsequently, the unit-cell was extended to a 10x10 array configuration in order to enable Two-dimensional (2D) beamsteering. This work yielded the fabrication of a prototype composed of four passive transmitarray lens, which were experimentally tested and characterised. Finally, a novel unit-cell based on a double square-slot intended aiming at active beamsteering was also studied and optimised in simulation environment.

From this work, it was demonstrated that transmitarray can be seen as feasible alternative to many traditional beamsteering techniques, such as phased antenna arrays, while reducing the RF burden of the overall system using only a single radiation source. This fact, allied with it's ease of integration, reduced cost and low-profile characteristics make transmitarrays a desirable solution for 5G and RADAR applications, among others.

Keywords: Transmitarray, Beamsteering, Frequency Selective Surfaces (FSS), 5G.

This page is intentionally left blank.

TABLE OF CONTENTS

LIST OF FIGURES

LIST OF TABLES

This page is intentionally left blank.

LIST OF ACRONYMS

1D	One-Dimensional.
2D	Two-Dimensional.
3D	Three-Dimensional.
BST	Barium-strontium-titanate.
CST	Computer Simulation Technology.
DC	Direct Current.
EM	Electromagnetic.
FSS	Frequency Selective Surfaces.
GPIB	General Purpose Interface Bus.
LHCP	Left-hand Circular Polarization.
MEMS	Micro Electromechanical Systems.
MM	Metamaterials.
MWS	Microwave Studio.
PCB	Printed Circuit Board.
PLL	Phase Lock Loop.
RADAR	Radio Detection And Ranging.
RF	Radio Frequency.
RHCP	Right-hand Circular Polarization.
Rx	Receiver.
SMD	Surface Mount Devices.
SMT	Surface Mount Technology.
SNR	Signal-to-Noise Ratio.
TA	Transmitarray.
Tx	Transmitter.
UC	Unit-cell.
VNA	Vector Network Analyser.

This page is intentionally left blank.

1

INTRODUCTION

1.1 BACKGROUND STUDY AND MOTIVATION

Electronic beamsteering is a concept that has gained huge interest in last years since it allows for the directing of the antenna beam towards a desired direction without the need for mechanical equipment. The most common method to perform beamsteering is by using phased antenna array [1–3]. An antenna array consist of a physical distribution of several antenna radiation elements, in the same plane, forming different patterns and configurations. By applying the correct phase difference between adjacent cells, it is possible to control the direction of the outgoing wave (or incoming wave when set for receiving mode), and thus perform beamsteering. However, the need for a different phase shifter for each of the cells proved to be costly and turned the system rather complex, which led to the search for new alternatives.

One of the favoured solutions that started to appear as a possible alternative to phased antenna arrays are transmitarrays. Transmitarrays are devices typically placed over a directional antenna aperture with the aim of altering its radiation properties, *e.g.* to perform focus, beamsteering or beamforming. Following the same physical principal of the phased antenna array, transmitarrays are often comprised of several similar unit-cells in which both frequency and phase response (phase-shift) depends on the unit-cell physical dimensions, and/or by loading discrete components such as capacitors, varactors or p-i-n diodes.

Depending on the the unit-cell design and on the discrete components employed in its composition, transmitarray can be used as passive device, e.g. as fixed beam lens aiming towards a specific direction, or as a reconfigurable (active) capable of adjusting the direction of the beam electronically.

In fact, electronic beamsteering using transmitarrays is both timely and topical in the context of the 5^{th} generation of mobile network (5G) [4] and Radio Detection And Ranging (RADAR) applications, particularly when these are applied to single radiating directive sources, such as a horn antenna. In the last years, several transmitarrays have been presented for 5G operating frequencies at sub-6 GHz band and at 28 GHz

1.2 OBJECTIVES

To this extent, this research work aims at the development of a Frequency Selective Surfaces (FSS)-inspired transmitarray for antenna beamsteering, for 5G and RADAR applications, at 28 GHz. This is sought to build upon the work carried out at 5 GHz [5]. Beamsteering using transmitarrays aims to eliminate the need of phase shifters by using artificial structured materials inspired on, for example, Metamaterials (MM) [6, 7] and FSS [8–11]. These structures exhibit resonant characteristics based on the appearance and geometries of the unit-cells. Furthermore, when using p-i-n or varactor diodes, it is possible to to modify the the capacitance value of the LC equivalent circuit of the unit-cell allowing for the control and tuning of the frequency response.

In this way, transmitarrays with such characteristics allow for an electronic control over beamsteering, overcoming the limitations imposed by the traditional array systems regarding the burden of Radio Frequency (RF) circuitry. This feature, when allied to the inexpensive Printed Circuit Board (PCB) manufacturing costs allow to a reduction of overall weight, power consumption and dimensions of the system, making these structures very attractive for inclusion in a large number of 5G and RADAR applications.

The main key objectives of this work are as follows:

- Review of the transmitarrays with beamsteering and polarisation control capabilities present in literature;
- Study of the theoretical models for One-Dimensional (1D) and Two-Dimensional (2D) beamsteering using a transmitarray;
- Familiarization with a full wave Electromagnetic (EM) solver (Computer Simulation Technology (CST) Microwave Studio (MWS));
- Dimensioning and characterisation of unit-cell based on FSS for passive transmitarray, using discrete capacitors in simulation environment;
- Prototyping and implementation of a passive transmitarray using the previously characterised unit-cell experimental tests of the passive prototypes;
- Study of the influence of the parasitic elements of the varactor diodes on the frequency response of the unit-cell and overall transmitarray capabilities;
- Dissemination of the work being performed in several conferences and journal publications with relevant scientific reputation.

1.3 DISSERTATION LAYOUT

Having the objectives in consideration, this dissertation is structured as follows:

Chapter 2 presents an extensive literature review and critical analysis on the topic of transmitarrays. Transmitarray based on different approaches and unit-cells (based on microstrip patches, MM and FSS) and employing p-i-n or varactor diodes, Micro Electromechanical Systems (MEMS) switches or even liquid crystals, are presented. Transmitarrays are divided in three categories: polarisation control, beamsteering and hybrids (transmitarrays that allow both polarisation control and beamsteering).

Chapter 3 presents the theoretical background for antenna beamsteering using a transmitarray. Both 1D and 2D beamsteering model approaches are presented herein.

Chapter 4 describes the methodology and characterisation of a passive transmitarray with two-dimensional beamsteering capabilities at 28 GHz. Firstly, several parametric studies in simulation environment are presented in order to ascertain the best dimensions for the unit-cell that allow better beamsteering results. Finally, a 5×5 array model composed of the designed unit-cells was characterised in terms of beamsteering performance.

Chapter 5 provides details on the practical implementation of the previously presented transmitarray, as well as additional simulations that were needed during the prototyping phase. In this chapter, the measurement setups and result analysis are presented.

Chapter 6 describes the simulation study carried on the unit-cell and, consequently, on the transmitarray, when the discrete capacitors considered previously are replaced by a more realistic model of the varactor diode. Two new unit-cells are then presented in order to perform beamsteering even when considering the parasitics of the varactor.

Chapter 7 is dedicated to the conclusions and final remarks of the work. Consideration is given regarding the topics that require further investigation as an extension of the work presented in this dissertation. Finally, the major contributions to the scientific community and knowledge are reported.

This page is intentionally left blank.

2

LITERATURE REVIEW

2.1 INTRODUCTION

Antenna beamsteering is a very useful and desirable technique in any wireless communication system since it allow to dynamically adjust the antenna pattern and consequently enhance Signal-to-Noise Ratio (SNR) [1]. Such feature is crucial to some applications that require tracking of objects and adaptation to dynamic scenarios with multipath and moving scatterers, e.g. base-station dynamic antenna alignment, wireless back-haul links auto-alignment due to pole swaying and twisting in the wind or mobile user tracking. Since such antenna systems is focusing their energy toward the receiver, it is increasing the useful received signal level and, thus, lowering the interference level. Hence, higher Signal-to-inference Ratio increases the capacity of the system and improves range and the coverage area.

The most traditional manner of implementing beamsteering is by using arrays of antenna [1–3]. However, the well known design limitations particularly regarding to the feeding network implementation, led to the introduction of alternative techniques to perform beamsteering. In 1986, *McGrath* firstly introduced in his paper [12] a microwave lens with focusing and scanning capabilities, by simply connecting two microstrip patch antennas using vias in both sides of a planar structure, forming a spatial array of microstrip patches, *i.e.* a transmitarray. Since then, transmitarray has been seen as a feasible alternative to phased antenna arrays and the focus of novel and extensive research nowadays.

Transmitarray [13–15] is the conventional name given to structures that can modify the original radiation pattern of a directional antenna source, *e.g.* horn antenna, when placed at a distance sufficiently away from its aperture. To the set composed by the structure and the radiating source, it is referred as transmitarray antenna [13–15]. Due to their electromagnetic properties, such structures are capable of modifying the characteristics of the incident EM wave emitted by the source, and perform beamsteering, focusing or even polarisation control, by re-transmission of the incident EM wave. Thus, one can imagine a transmitarray acting, in a sense, like a lens, allowing to pass-through the incident wave with an alteration (or not) of its direction of propagation, as depicted in Fig. 2.1a. The direction to which the incident wave is being re-radiated depends on the design of the structure. These

structures are commonly composed by several resonant unitary elements (unit-cells) with a spatial periodicity forming a planar array [13–15]. The unit-cells are typically based on simple microstrip patches, or inspired by MM [6, 7] and FSS [8–11]. From a practical point of view, since transmitarray structures are mostly implemented using PCB technology [13–15], by etching the unit-cell geometries on a copper covered substrate, they benefit from being planar and thus easy to integrate with other radio peripherals. Furthermore, they are compatible with Surface Mount Technology (SMT) allowing to reduce the size of assemblies, and finally, since they have the electromagnetic feeding source separated from the beamsteering network, they offer higher degree of modularity to the system as opposed to traditional antenna array. Thus due to their design simplicity and, more importantly, due to the low manufacture costs, they have been extensively utilized for numerous antenna applications.

In order to achieve reconfigurability and enable features, such as electronic beamsteering, polarisation control or frequency tuning, transmitarray are typically enhanced by using p-i-n diodes, varactor diodes, RF or MEMS switches or manufactured using tunable substrates as liquid crystal or graphene. However, each of these methods present advantages and disadvantages, *e.g.* p-i-n and varactor diodes are widely utilized in transmitarray designs from low RF to around 30 GHz, mostly due to their size, easy integration in PCB and low cost. However, they are limited when operating at high frequencies (above 30 GHz), with insertion loss proportional to the frequency of operation that arise from their intrinsic parasitic parameters (series resistance, capacitance and inductance). RF and MEMS switches are typically more expensive than p-i-n/ varactors and prone to failure over time, due to the wear and tear of the mechanical parts. Alternatively, tunable dielectric materials, *i.e.* materials that can have their electromagnetic properties (in particular ϵ_r) manipulated by an external stimulus (bias or voltage), such as liquid crystal and graphene are also employed for transmitarray implementations [16–22]. Furthermore, while liquid crystal technology have been successfully employed in transmitarray designs [16], it is more commonly used in reflectarray implementations [23–26] or as grounded substrate for conventional microstrip antennas [27–29]. Graphene substrates, on the other hand, are typically used at THz frequencies due to their unique electronic properties as reported in [30], even though applications in antennas design at micro- and millimeter-wave frequencies, have already been reported in [31].

The research on transmitarray has always been paired to the one on reflectarray [32, 33]. Reflectarray, which operating principle is depicted in Fig. 2.1b, makes use of the reflection principle (based on Snell's law [32, 33]) to modify the properties of the re-transmitted EM wave. In fact, the most significant difference between a transmitarray and reflectarray is that, in the latter, all power is re-radiated independent on the frequency or cell design. If the unit-cells are not matched to the

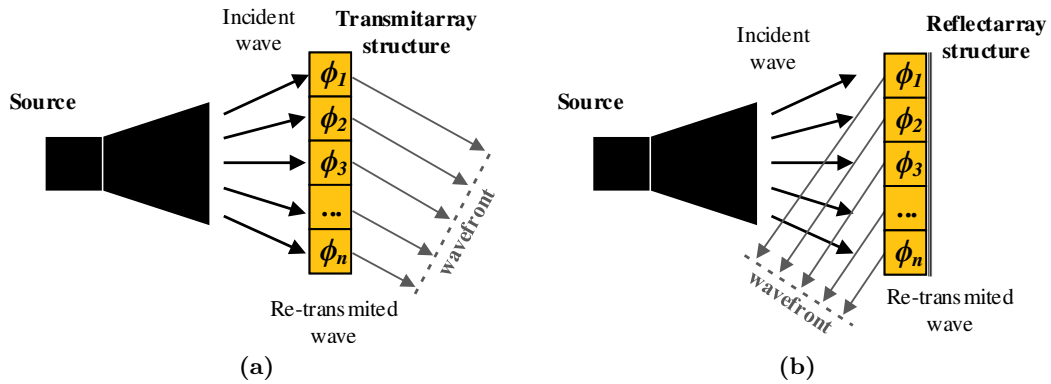

Figure 2.1: Generic model of (a) a transmitarray and (b) a reflectarray antenna.

frequency of operation, the elements will have small effect on the array response and the reflecting ground plane will predominate. In the worst case scenario, the reflected wave could have the same direction of the original one [32, 33]. On the other hand, for a transmitarray, if the structure is not well matched to the free-space or if the unit-cells are not adapted to the frequency of operation, the incident EM wave will be totally reflected back, resulting in no transmission through the structure [13, 14]. Therefore, a transmitarray is desirable to be the most "transparent" as possible, introducing very low loss so the EM field of the propagating wave is not severely attenuated, whereas the reflectarray is desirable to be a perfect reflecting surface so the incident wave can be entirely reflected.

However, although reflectarray have been successfully implemented in [15, 32–38], the feed blockage remains a challenge in implementation of such type of devices since the feeding source is on the same side of the radiated field. This may be a challenging depending on the final application that can be overcome with the use of a transmitarray.

2.2 TRANSMITARRAY FOR ANTENNA BEAMSTEERING

Several examples can be found in the literature for transmitarray aiming antenna beamsteering. They comprise the use of different materials, unit-cells designs and implementation approaches. However, there is one requirement that must be satisfied to use such structures to steer the main beam of an antenna radiation pattern. The unitary element that composes the transmitarray must have transmission phase that can be varied (tunable) up to 360° (as will be explained in section 3.3), while the transmission magnitude (desirably) remains constant over the bandwidth,. Therefore, this section is focused on the review of transmitarray structures and unit-cell elements, with reconfigurable capabilities that enable electronic beamsteering.

2.2.1 *Reconfigurable based on microstrip patches*

Particularly in [39], a reconfigurable transmitarray for beamsteering is proposed. The device is composed of a set of patch antennas placed on each side of the array structure and connected by an electronically tunable phase-shifter, where the innovation of the work relies on. The phase-shifter is developed in transmission line technology and consists of a microstrip directional coupler terminated with reflective LC circuits, whose capacitance (C) is controlled by a varactor diode. Consequently, by tuning the value of C, it is possible to selected whether the terminations of the coupler are open- or short- circuit and thus, control the phase-shift between the input and the output of the transmitarray. Nevertheless, this solution turned out to be limited in terms of phase range and since several couplers are cascaded together to overcome this issue, the size and complexity of the phase-shift network is consequently increased. This forced a large separation between the radiating elements, that were arranged in groups of 4 elements and separated by 1.4 wavelengths, leading to the reduction in the scan capability and to the appearing of grating lobes. Therefore, a maximum of 9° of angular shift is reported on the azimuth plane. The proposed solution presents 700 MHz of bandwidth and 3 dB of insertion losses but such values are advertised for the phase-shifter alone and not for the complete transmitarray.

Remarkably in their work, *Lau* and *Hum* [13, 40–43] have introduced several models of active unit-cells and of electronically controlled transmitarray. Specifically aiming antenna beamsteering, it is presented and characterized in [40] and further improved in [41] a transmitarray element (Fig. 2.2a) that consists of two microstrip patches on either side of a ground plane coupled to a small slot aperture. Each patch is split in half with a small gap in between, and varactor diodes inserted to connect the two halves, while another varactor diode is inserted at the center of the slot, connecting the two sides of the slot. Together, all these parts act as three coupled tunable resonators that provides a variable phase-shift over 360° with 3 dB of insertion losses, as reported in [41]. However, the losses are slightly increased to 4.8 dB (over the same bandwidth), when the proposed element is composing a 6×6 array and the biasing network to control the varactors are included, as depicted in Fig. 2.2b [41]. Nonetheless, the developed prototype achieved $\pm 25^\circ$ of electronically controlled beam scanning, in azimuth and elevation planes independently, with a broadside directivity of 20.8 dBi.

As alternative, a different unitary element is proposed and characterized by the same authors in [42]. The unit-cell for transmitarray applications explores the properties of proximity-coupled feeding and aperture coupling [1]. In this solution, the array element is implemented with microstrip patches in both sides of the

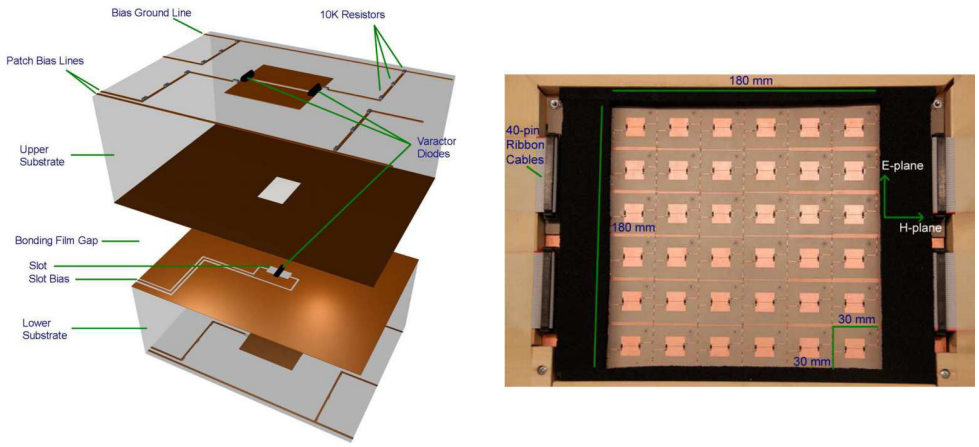

(a) **(b)**

Figure 2.2: (a) Reconfigurable element (exploded-view) and (b) respective transmitarray prototype (images extracted from the work presented in [41]).

structure separated by a ground plane. Each patch fed a differential microstrip transmission line by mutual coupling. In one of the sides, possess a differential bridged-T phase-shifter composed by varactor diodes and Direct Current (DC) blocking capacitors. Both sides of the structure are further interconnected also by aperture coupling through two open slots etched in the ground plane. According to experiments realized on a single unit-cell using the waveguide method, which consists of a sample of the unit-cell enclosed between two waveguide flanges, it is notably achieved a tunable phase range of around 425° and insertion loss in average of 3.4 dB at 4.86 GHz. This model is however limited by the narrow bandwidth of the radiating elements and such drawback is mitigated, on a final prototype by employing a stack of microstrip patches. The final array element exhibits insertion losses of around 3.6 dB with a phase range over 400°, but the bandwidth was increased from 100 to 500 MHz at the same central frequency. Subsequently, a 6×6 reconfigurable transmitarray composed of active elements of [42] is finally presented and evaluated in terms of beamsteering performance in [43]. The prototype of the transmitarray provides a scanning range of $\pm 50°$ in both elevation and azimuth planes, with 2.2 dB of insertion losses and 10% bandwidth (500 MHz) at 5 GHz.

Moreover, in [44], a novel unit-cell design is proposed and characterised for an electronic control of the wave direction using a transmitarray. It is composed of a passive microstrip patch antenna with U-shape slot etched on the reception plane, and an active patch with an etched O-shape slot in the re-transmission plane, as depicted in Fig. 2.3a. The active O-shape is loaded with two p-i-n diodes (and in an alternative design with RF - MEMS) that allow to control the transmission phase by alternatively activating diode states. A 15% of bandwidth and around 3 dB of insertion losses at 10 GHz are reported experimentally on a single unit-cell, evaluated using the waveguide method also employed in [42]. Later in [45], the same unit-cell

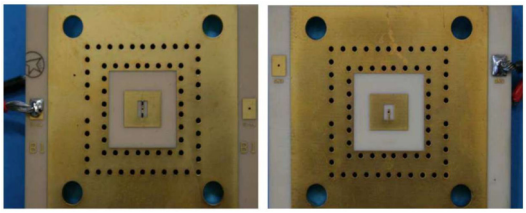

(a)

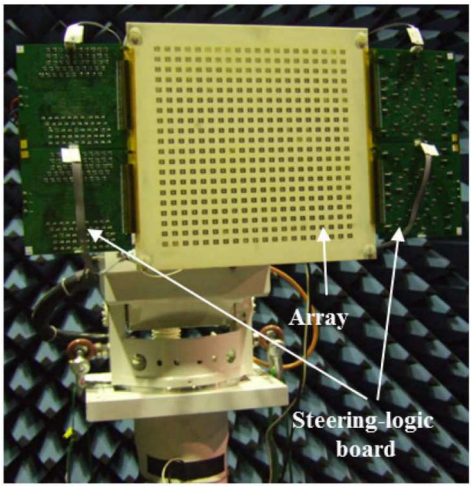

(b)

Figure 2.3: (a) Unit-cell design and (b) transmitarray prototype for antenna beamsteering (images extracted from the work presented in [44] and [46], respectively).

design using MEMS presents a bandwidth of 16% but 4 dB of insertions losses. In [46] the authors presented a full characterization of a 20×20 transmitarray comprising 800 p-i-n diodes and the respective feeding mesh. The prototype is depicted in Fig. 2.3b. The authors state that the proposed transmitarray exhibits a 2D beamsteering capability with maximum ranges of $\pm 40°$ in elevation and $\pm 70°$ in azimuth.

Another unit-cell for beamsteering transmitarray at Ka-band based on p-i-n diodes is presented in [47]. The paper starts by characterising by simulations an novel unit-cell design. In particular, this novel unit-cell design allows for a 2-bit phase resolution and has an overall size of $5.1 \times 5.1 \times 1.3mm^3$ ($\lambda/2 \times \lambda/2 \times \lambda/8$ at 29 GHz). The unit-cell is composed of six metal layers printed on three substrates as shown in Fig. 2.4b, of which the ones at the edges are O-slot rectangular patch antennas loaded with two p-i-n diodes for phase control. Similar to other cases already presented [44, 46], the p-i-n diodes in each of the antennas are biased in opposite states (one p-i-n diode is ON while the other is OFF). By choosing which diode is ON at a given time, a $180°$ phase-shift is achieved. Therefore, by combining the different states of the receiving and transmitting layers, a total of four phase.shifts can be achieved ($0°$, $90°$, $180°$ and $270°$). The presented unit-cell is used to implement a 14×14 element transmitarray in simulation environment whose beamsteering range is reported up to $-40°$, as shown in Fig. 2.4b.

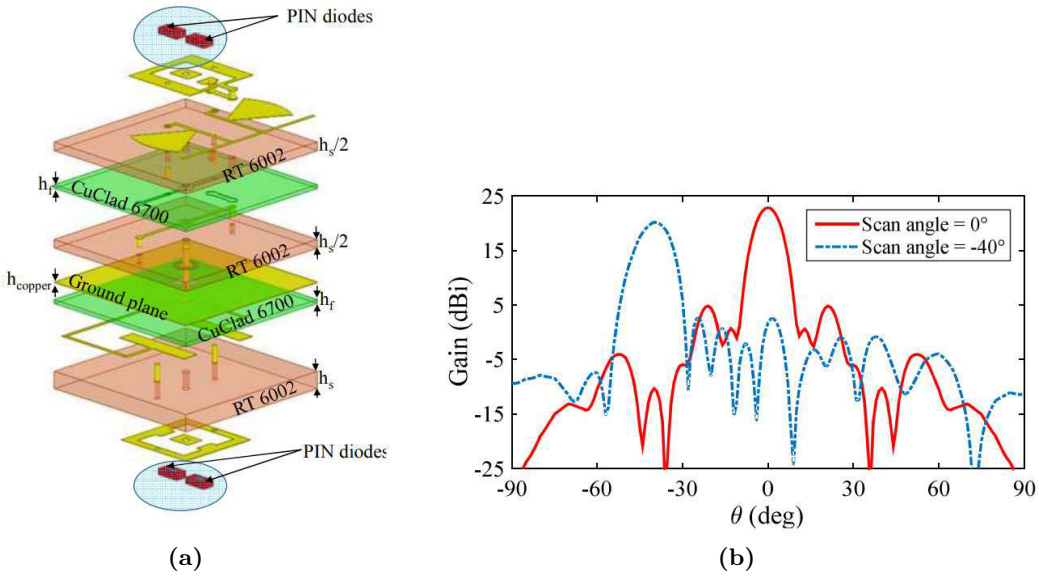

Figure 2.4: (a) Schematic view of the 2-bit unit-cell and (b) simulated radiation pattern for two angles (images extracted from the work presented in [47]).

More recently, in [48] a new unit-cell for a beamsteering transmitarray is presented. Each cell is comprised of four stacked Rogers RO4350B double sided layer, as depicted in Fig. 2.5a. Since one pair of layers (sub-element) can only achieve 180°, this arrangement has to be replicated in order to achieve the desired 360° of phase shift. Varactor diodes are used in every layer to control, electronically, the element phase-shift. Although the paper reports a bandwidth of 1 GHz for the unit-cell at 24.6 GHz, this value is defined by the frequency range in which the phase-shift is above 360 degrees, and not from the S_{11}/S_{22} filtering response as normally characterized in this type of work. This unit-cell, exhibits then a total insertion loss of around -5 dB obtained in simulation and -12 dB obtained experimentally. Finally in [48] a 6×6 transmitarray composed of the aforementioned unit-cell has been built (Fig. 2.5b). This transmitarray is able to steer the main beam direction up to $\pm 50°$ in both the azimuth and elevation planes, at 24.6 GHz, with a maximum attenuation of 17 dB at the extremes of the steering interval.

2.2.2 *Reconfigurable based on tunable metamaterials*

Transmitarray composed of MM to perform antenna beamsteering are also reported in the literature. Metamaterials are artificial man-made structured materials able to produce electromagnetic properties (permittivity, permeability and refractive index) which are unusual or non-existent in nature [6, 7] and such properties can be explored for transmitarray designs.

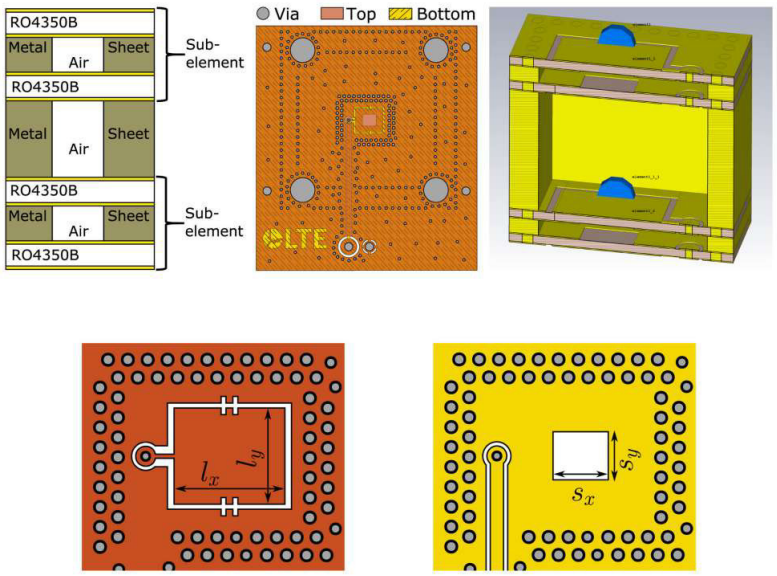

(a)

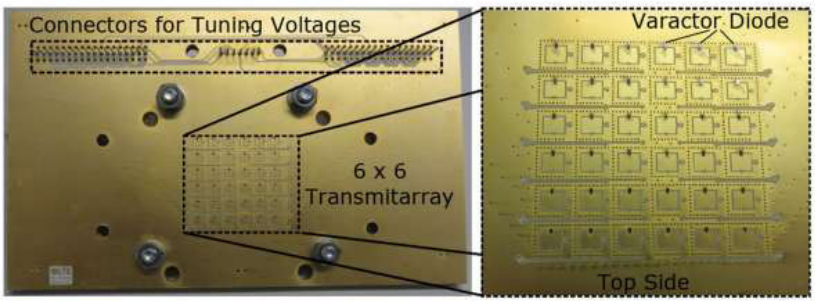

(b)

Figure 2.5: (a) Unit-cell design and (b) top view of assembled 6x6 transmitarray prototype (images extracted from the work presented in [48]).

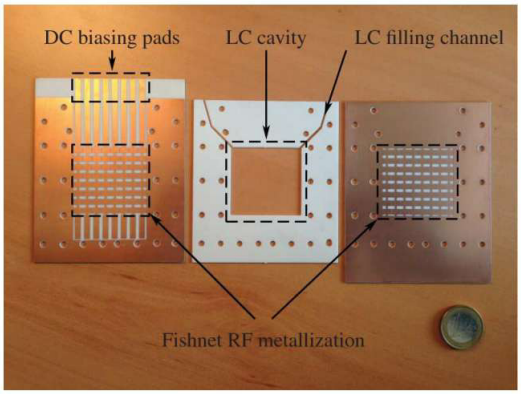

Figure 2.6: Prototype of a single opened fishnet unit-cell layer (images extracted from the work presented in [16]).

It is the case of the work described in [16], [49] and [50], where 1D beamsteering, *i.e.* main lobe limited to steering in a single plane, is demonstrated using such type of materials. These works [16, 49, 50] suggest new steerable antennas by using controllable MM (electronically reconfigurable) to form the transmitarray. Although implemented with different resonant unit-cell designs, they all respect the same physical principle: tunable refractive index structures are utilized to electronically control the direction of the outcoming wave. The steering is achieved when the refractive index of the MM structure is tuned, leading to a progressive phase distribution along the structure, acting as a linear phased array.

For example, in [16] the authors have developed and characterized an artificial gradient-index metamaterial by designing a fishnet structure on a liquid crystal substrate. The transmitarray was practical validated against measurements conducted at 27.5 GHz. A beamsteering angular range limited to $\pm 5^{\circ}$ was achieved by varying, in a gradient manner, the bias of each array column. According to the authors, the yielded angular range can be enhanced by staking more layers of the one depicted in Fig. 2.6.

In [49] and [50], the authors have followed an alternative approach to design their transmitarray. Both presented structures are composed of staked layers of periodically printed sub-wavelength metallic resonators with embedded microwave varactors. By adjusting the varactor diode, the resonant characteristics of the unit-cell is modified controlling, in fact, the associated phase-delay between the first and the last layer of the transmitarray. Consequently, the associated effective refractive index of a single transmitarray element is being adjusted. Accordingly, if a progressive phase between adjacent elements is applied through the array in order to perform beamsteering, the metamaterial exhibits a gradient index of refraction, when seen as an whole.

Therefore in [49], 6 stacked layers of a double-layer I-shaped unit-cell (Fig. 2.7a) are suggested as array element, exhibiting 360° of phase-shift at 1.6 GHz while the

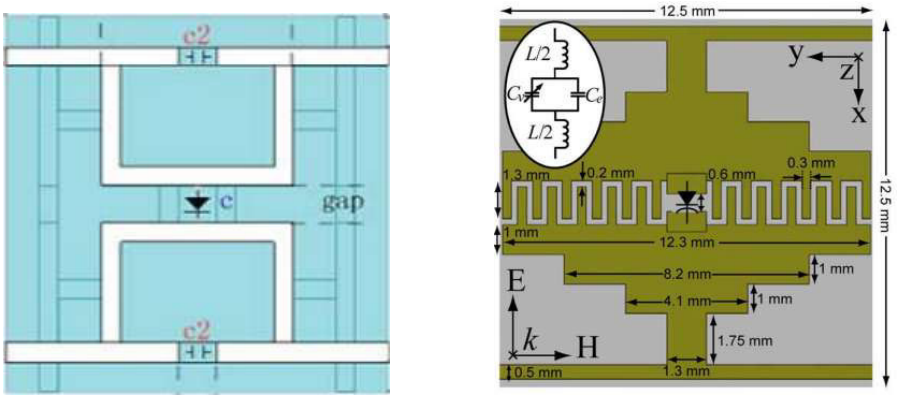

(a) **(b)**

Figure 2.7: Metamaterial unit-cells for transmitarray antennas presented by (a) *Yongzhi S. et. al.* and by (b) *Jiang T. et. al.* (images extracted from the work presented in [49] and [50], respectively).

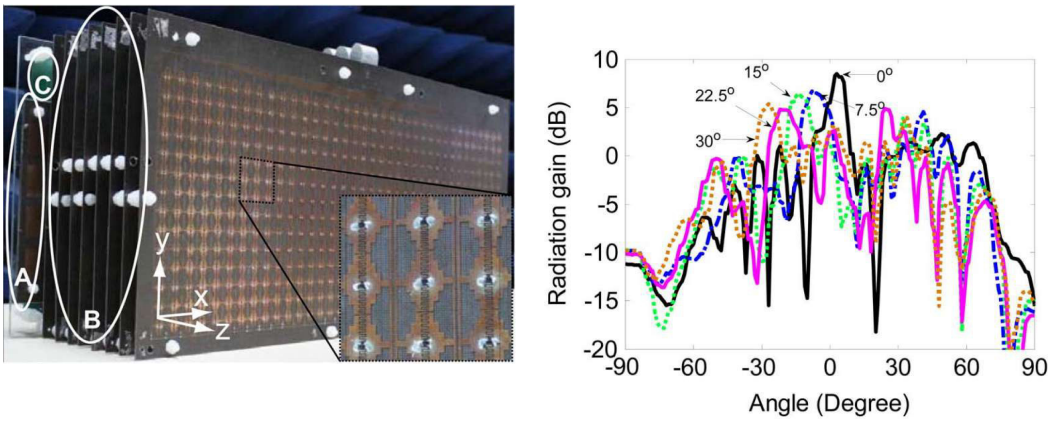

(a) **(b)**

Figure 2.8: (a) Prototype of the MM beamsteering antenna and (b) measured radiation pattern for different steering angles (images extracted from the work presented in [50]).

varactor is tuned from 0.1 pF to 1.9 pF, with insertion losses of 4 dB (averaged). Bandwidth is not referred by the authors. A continuous scanning range of $\pm 30^\circ$ in the azimuth plane is achieved using a full wave simulator. Although it is stated that experimental results obtained on a prototype are consistent with simulation ones, the paper lacks a more elaborated and physically grounded analysis of the results.

Notably in [50], a complete characterization of a metamaterial transmitarray composed by the unit cell presented in Fig. 2.7b was performed. In addition to the transmitarray, an array of microstrip patch antennas was also developed to serve as feeding source. The prototype, implemented on a stacked layer structure (Fig. 2.8a), presents an angular steering range of $\pm 30^\circ$ in azimuth verified under experiments at 4.7 GHz. Some samples of radiation pattern are demonstrated by the authors in their paper and illustrated in Fig. 2.8b.

Although introduced as MM by analyzing the refractive index of the array element, it can be noticed that such structures are in fact FSS. While the unit-cell presented in [49] exhibits a low-pass filtering frequency response, the unit-cell of reference [50] possesses a band-pass filtering type. Herein, is when the term metamaterials could be misleading due to large ambiguity of the definition.

2.2.3 *Reconfigurable based on FSS*

Frequency selective surfaces [8–11] are, per se, a timely topic on the field of (antennas and) propagation that have been studied for years. A FSS is a spacial filter that exhibits distinct resonant filtering characteristics *e.g.*: band-pass, band-stop, high-pass or low-pass, that depend on the format and on the dimensions of periodic resonant geometries etched over a metallic coated substrate [8–11]. As a spacial filter, these structures are able to allow or block the propagation of an incident EM wave within a specific frequency band and even control its propagation phase.

Much of the work about FSS relies on the study and development of novel unit-cell designs for EM blockage (shielding) or radio coverage enhancement [8–11]. However, new applications have recently emerged by exploring the use FSS in various transmitarray implementations [51–59] and in novel antenna designs [60–62].

For example in [51], a wide-band transmitarray is suggested by using a FSS of double square rings unit-cells. The authors have demonstrated that the phase-shift introduced by the transmitarray can be varied by simply modifying the physical size of the squares, and such can be further improved by stacking several layers of FSS on top of each others. In fact, the concept of stacked layers separated by an air gap is widely used for transmitarray implemented with FSS since it allows to increase both the bandwidth and the transmission phase of the structure, as thoroughly reported in [13, 51, 54, 57, 58].

In particular, some examples can be found in [52–56] by presenting reconfigurable transmitarray of FSS for antenna beamsteering. The majority of the work utilizes varactor diodes to electronically control the capacitance of the equivalent LC circuit that characterizes the resonant unit-cell design, as presented by *Russo et. al.* in [52–54]. In their work, a tunable pass-band FSS suitable for beamsteering operations is proposed. The suggested FSS, depicted in Fig. 2.9a, is evaluated by simulations in [52, 53] and experimentally characterized in [54], also using the waveguide method (Fig. 2.9b), previously described. The proposed structure is capable of bandwidths ranging from 1% to 10% (with a few modifications in original design) at 4 GHz, with a transmission amplitude that remains above 3 dB within the varactor tuning range. Although the transmission phase obtained from experiments

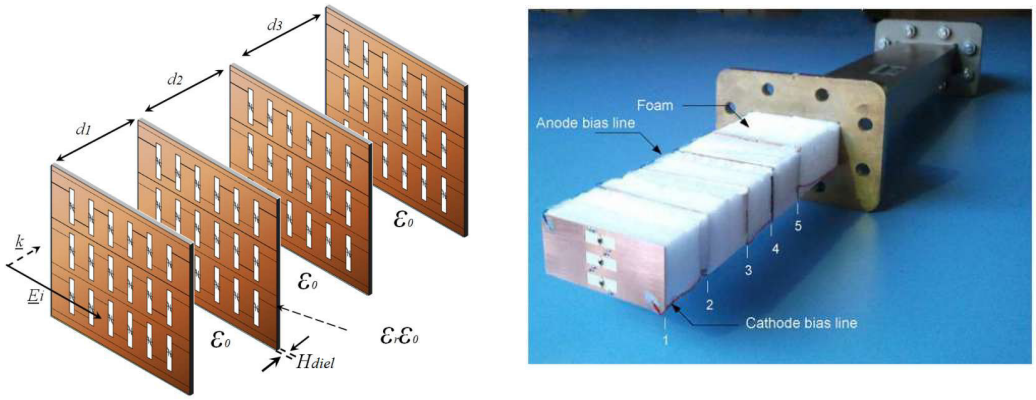

(a) **(b)**

Figure 2.9: (a) FSS transmitarray model and (b) respective unit-cell prototype evaluated using the waveguide method (images extracted from the work presented in [53] and [54], respectively).

varies by approximately 360° over the whole bandwidth, making this design suitable for beamsteering, the paper does not include the implementation of a complete transmitarray and respective beamsteering characterization.

In [55], an active FSS based on the traditional squared-slot design with band-pass filtering characteristics is implemented for antenna beamsteering, as depicted in Fig. 2.10. Varactor diodes are used to tune the FSS and control the phase-shift, with range up to 360°, of a structure composed of 5 stacked layers. In fact, the authors have demonstrated on a physical prototype, illustrated in Fig. 2.10a, that through different configurations of the bias voltages applied to the varactors, a gradient phase distribution along the transmitarray can be utilized to steer the radiation pattern of a horn antenna. This corroborates with the facts presented for MM transmitarray introduced in last section. Although the work show its merits by presenting a tunable steering range of ±30° in both azimuth and elevation plans at 5.3 GHz, as depicted in Fig. 2.10b and Fig. 2.10c respectively, it is a fact that such scanning angle can only satisfy one steering direction at the time. Therefore, two-dimensional beamsteering, *i.e.* steer the main lobe to a direction with two spatial components as presented in Section 3.3, is still unachievable with this device.

Alternatively in [56], a tunable FSS with beam steering capability is presented. The FSS is used as a transmitarray with a bandpass characteristic centered at 12 GHz. The novelty of the work relies on the FSS design which is composed of capacitive (parallel electrodes) and inductive (vertical wires) structures printed on a Barium-strontium-titanate (BST) thick-film ceramic, as illustrated in Fig. 2.11. The tunability is performed due to the properties of the BST substrate that can be tuned by applying an external electrostatic field across the material, and not by using discrete components such varactors or p-i-n diodes. By applying a DC field between the electrodes of the capacitor, the effective permittivity is reduced resulting also

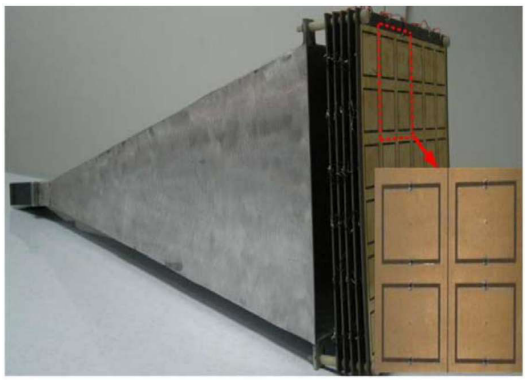

(a)

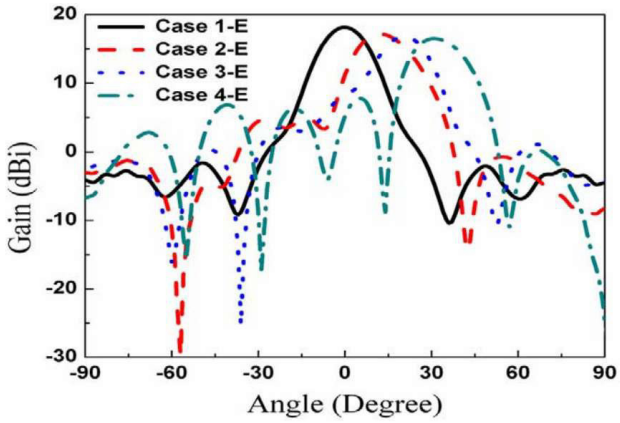

(b)

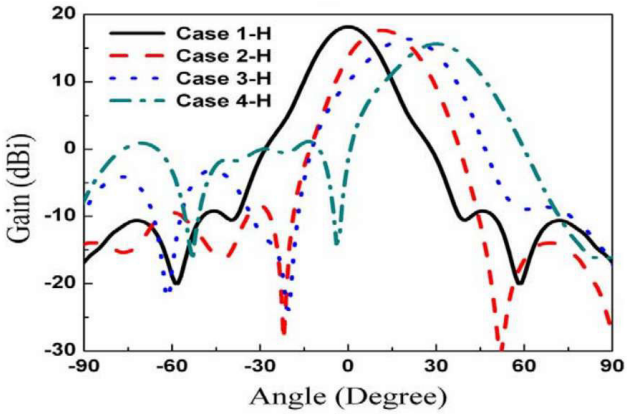

(c)

Figure 2.10: (a) 6×6 transmitarray prototype, (b,c) measured radiation pattern in azimuth and elevation planes, respectively (images extracted from the work presented in [55]).

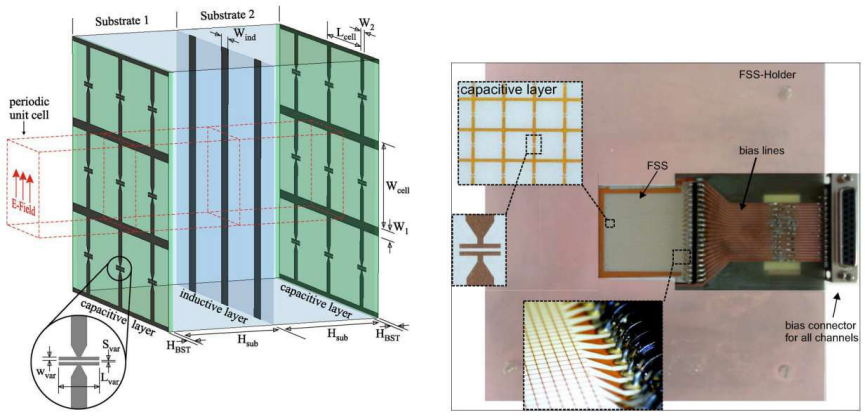

(a) **(b)**

Figure 2.11: (a) FSS transmitarray model and (b) respective transmitarray prototype (images extracted from the work presented in [56]).

in a capacitance reduction. Experiments realized on a 40×40 FSS transmitarray (Fig. 2.11b), report a maximum phase difference of $121°$ at 12 GHz when the bias voltage is ranging from 0 V (untuned state) and 120 V (maximum tuning state). Within such voltage range, the main beam of a feeding horn antenna is steered up to $\pm 10°$ in the azimuth plane, due to the low phase-shift ($121°$) produced by the structure. Although showing its merits, the proposed solution is one of a type in the literature, possible due to the impractical voltage values necessary to apply for tuning the structure and perform 1D limited beamsteering, in comparison with other state-of-the-art proposals.

To withdraw such limitation, a reconfigurable transmitarray model for 2D beamsteering was presented in [57, 58]. The transmitarray follows the phase distribution proposed by the theoretical model presented in section 3.3 in order to enable antenna beamsteering in two dimensional planes. With this mindset, it is presented in [57] and further in [58] the characterization of a FSS transmitarray with controlled beamsteering output direction in the two main antenna planes (azimuth and elevation). Firstly in [57], the theoretical model for 2D beamsteering has been applied on a passive stacked-layer FSS inspired transmitarray. Based on a square-slot pass-band unit-cell layout (as in [55]), the 2D beamsteering model was tested for several beamsteering angles on a 5×5 transmitarray with 5 stacked layers separated by an air gap, at 5.35 GHz. The paper, which also includes a parametric study to evaluate the ideal layer separation distance and the ideal number of layers necessary to achieve a desired phase-shift, reports beamsteering angles up to $\pm 25°$ in both elevation and azimuth planes with $3°$ of error between simulation and experimental validating the theoretical 2D model. Although beamsteering is set by the value of each of the 50 discrete SMT capacitor loaded in each layer, the several output angles were achieved by hand-soldering the capacitors for each angular configuration.

Subsequently in [58], the latter model has been improved to enable electronically reconfigurable beamsteering. In the addition to through-layer *vias* per unit-cell, a sixth layer has been added to accommodate the feeding network, as depicted in Fig. 2.12a. Varactor diodes replaced the discrete SMT capacitors used in the passive transmitarray of [57]. A beamsteering driver has been developed to control, individually, the overall capacitance value of each of the 25 cells of the transmitarray. As result, beamsteering angles up to $\pm 28^{\circ}$ in azimuth and $\pm 26^{\circ}$ in elevation have been accomplished with the physical prototype of Fig. 2.12b. Two samples of measured radiation pattern are depicted in Fig 2.12d and Fig. 2.12e, for (15°,15°) and (25°,25°), respectively. The reconfigurable transmitarray exhibits insertion loss of 1.6 dB and 4.3 dB in simulation and experiments, respectively. This compares with the experimental results obtained in the passive model by presenting approximately 1.5dB of excess loss at 5.2 GHz, due to the intrinsic parasitic effect of the selected varactor diodes.

The transmitarray presented in [58] was also studied as a redirecting metasurface for outdoor-indoor radio coverage enhancement by the candidate in a moment prior to the development of the work presented in this dissertation [63]. This was done by inserting the transmitarray in a wall (hereafter denominated by smart wall), as depicted in Fig.2.13a, instead of directly placing it in the vicinity of the supporting antenna. Measurement results showing the effect of the smart wall when compared to free space and a metallic plate are presented in Figs. 2.13b and 2.13c, for frequency and azimuthal angle sweep, respectively. The band-pass filtering effect of this transmitarray can be clearly seen in Fig.2.13b (filter centre frequency around 5.2 GHz). By controlling the smart wall with a computer, it is possible to redirect the main beam of the incoming wave to any direction in both planes beyond the wall. As shown in Fig. 2.13d, the main lobe of the incoming wave was successfully shifted electronically from 0° to 10°, 20° and 30° in the azimuthal plane.

Another design of FSS-based unit-cells for beamsteering transmitarray is presented in [59]. The unit-cell is based on a C-patch and ring slot loaded with p-i-n diodes (Fig. 2.14) and is composed of two identical substrates with dimensions of $14 \times 14\ mm^2$. The ring slot is loaded by a rectangular gap and is placed just beneath the gap of the C-patch. In this particular unit-cell, the C-patches act as the receiver and transmitter, while the ring slots act as a phase shifter. The phase shift between the receiver and transmitter can be controlled by modifying the length of the ring slot gaps. In order to change the associated electrical length, each gap is loaded with p-i-n diodes that allow a 180° of phase shift at 11.5 GHz. However, since both terminals of the p-i-n diodes are short-circuited, a second rectangular gap was introduced in the cell presented in Fig. 2.14. This gap is 0.2 mm and is loaded with three 100 pF capacitors in order to the current flow through the gap. The first unit-cell was then simulated in a 12×12 transmitarray to verify its beamsteering

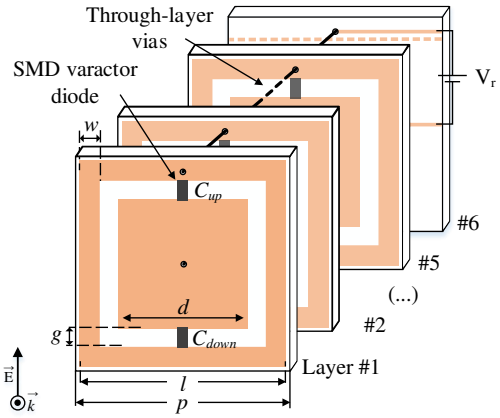

(a)

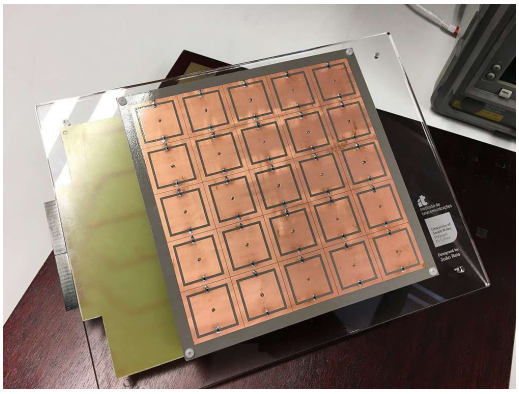

(b)

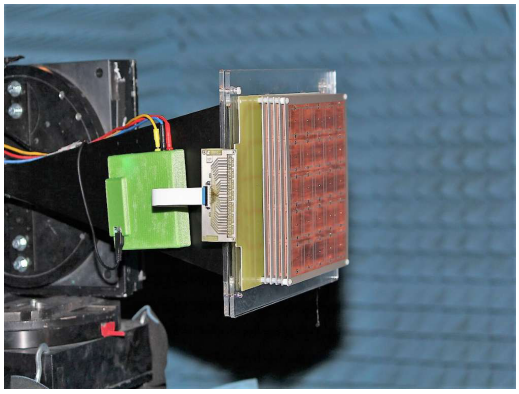

(c)

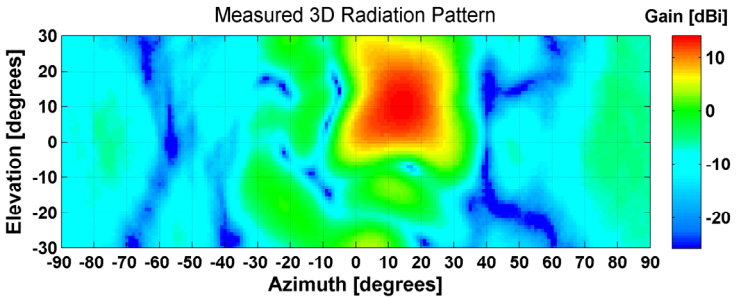

(d)

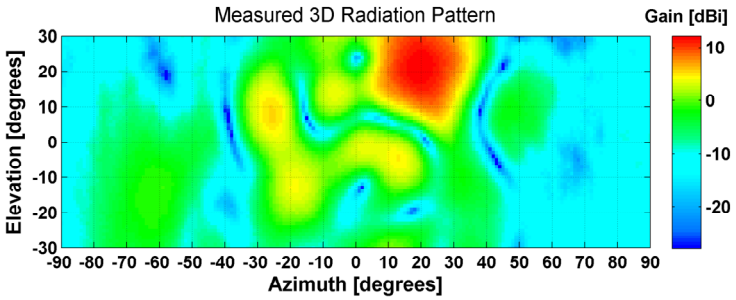

(e)

Figure 2.12: (a) Unit-cell model, (b,c) 5×5 transmitarray prototype and (d,e) measured radiation pattern for (15°,15°) and (25°,25°), respectively. (images extracted from [58]).

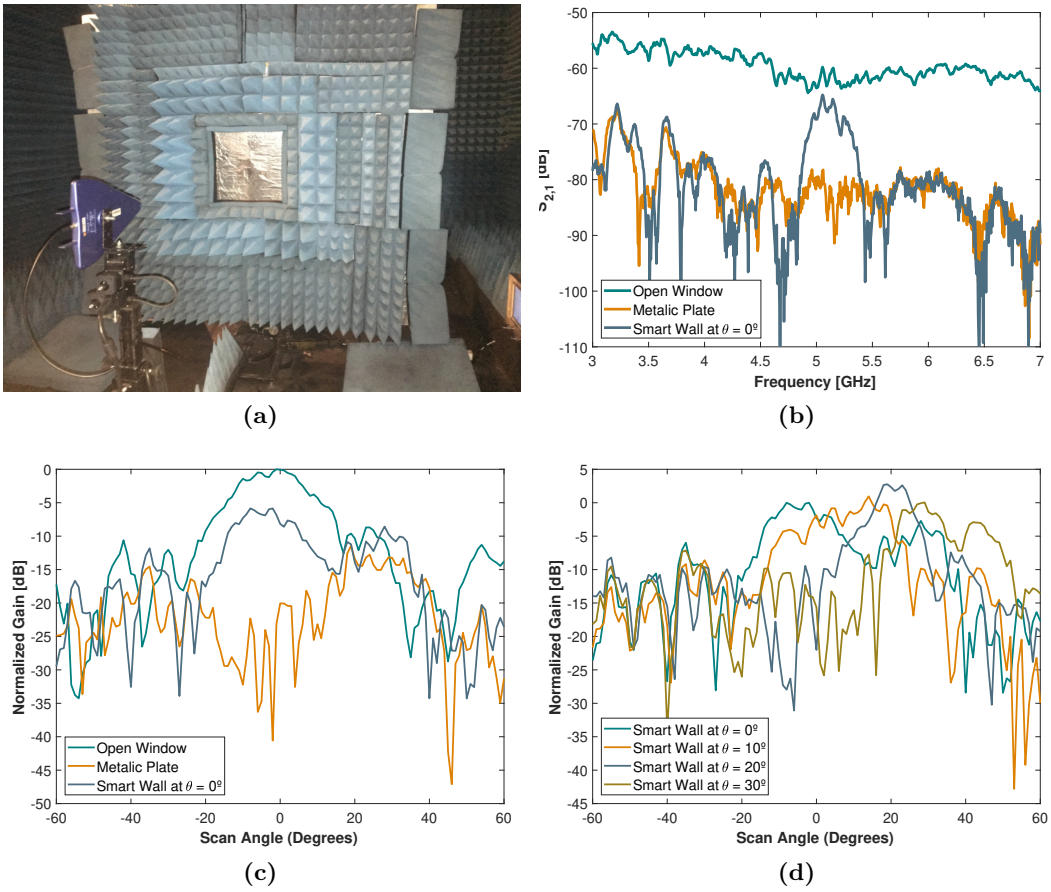

Figure 2.13: (a) Measured radiation power for each setup from 3 to 7 GHz, (b) measured radiation pattern for each setup from -60° to 60° at 5.2 GHz and, (c) measured radiation pattern for the smart wall tuned to 0°, 10°, 20° and 30°.

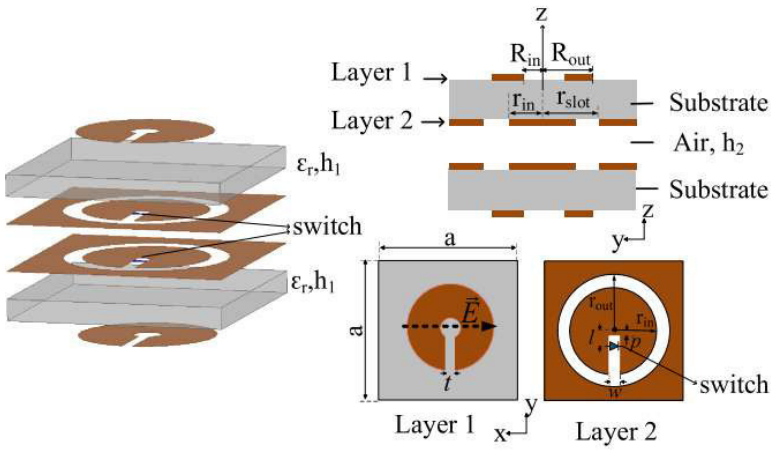

Figure 2.14: Geometry of transmitarray unit-cell (image extracted from the work presented in [59]).

capabilities. For each of the cells a single bias line is needed to control the ON/OFF state of the p-i-n diodes. Simulation results show that, at 11.5 GHz, a $\pm 40°$ in both azimuth and elevation planes is achieved. At the moment there are not experiments on this structure.

2.3 TRANSMITARRAY FOR POLARISATION CONTROL

Several transmitarray have been presented in last section all aiming antenna beam-steering. However, transmitarray have also been used to control the polarisation of the re-radiated EM, as the ones described as follows.

First introduced in [64] and further in [65], the authors have presented a transmitarray with the objective of controlling the polarisation of the wavefront. The proposed structure is based on microstrip patch antennas, whose elements in the outer side of the structure are physically rotated ($\alpha = 0°$, $90°$, $180°$, and $270°$) relative to the patch feeding point), to tilt the polarisation of the re-transmitted wave. The implemented unit-cells and the respective transmitarray are depicted in Fig. 2.15 [65]. The polarisation of the re-radiated wave is forced by tilting mechanically of each unit-cell enabling the developed transmitarray to produce a circularly polarised wave. Since the polarisation control is performed through sequential rotation and no other mechanism was implemented to automatically modify the properties of the transmitarray, rather than mechanical movement, the suggested model is considered a passive device.

Following the same approach, a novel passive transmitarray was latter introduced in [66] by the same research group. This particular device exhibits an enhanced unit-cell also based on microstrip patch with etched corners. A prototype of the

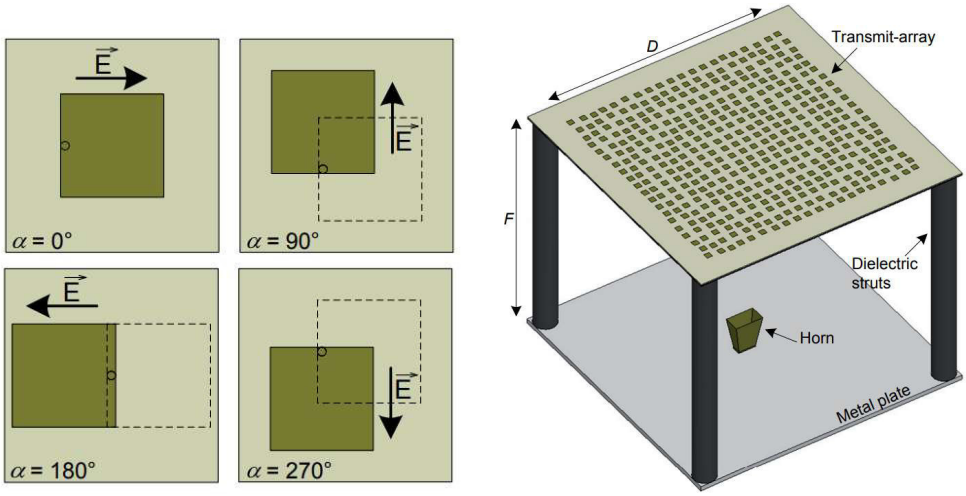

Figure 2.15: (a) Patch unit-cell and (b) transmitarray model for polarisation control (images extracted from the work presented in [65]).

device measured a broadside gain of 22.8 dBi at the simulated frequency with a 3 dB bandwidth of 20% in Right-hand Circular Polarization (RHCP) and 3 dB axial ratio with bandwidth of 24.4%.

With a novel unit-cell design and following a slightly different methodology, a novel transmitarray was introduced by *Pfeiffer* and *Grbic* in [67]. This design was implemented by using cascading metallic surfaces to provide polarisation and wavefront control. Two transmitarray were developed and tested experimentally both based on a quarter-wave plate design that transforms a linearly polarised incident wave into a circularly polarised transmitted wave, by exploring the phase shift created between both faces of the structures. Since the phase difference between two orthogonal E-field components is a quarter of the wavelength (90°), when an incident field is linearly polarised at (45°) relative to its axes, the quarter-wave plate converts the transmitted field to circular polarisation.

In [68] another polarisation controlled transmitarray has been presented by stacking together several layers of rectangle ring slot unit-cells, separated by an air gap. Remarkably, the proposed device is capable of realizing Left-hand Circular Polarization (LHCP) and RHCP, and linear polarisation, when excited by a linearly polarised feeding source (*Vivaldi* antenna). This is achieved due to the enhanced phased control given by the stacked layers but also by varying the size of the unit-cell throughout the array. By varying the X and Y dimensions of the rectangle ring slot element, transmission magnitude and phase shift for both polarisations can be achieved. Therefore, it is possible to perform a change in polarisation by adjusting the rotation angles of the feeding antenna through the phase of the linearly polarised incoming wave.

The main difference in the underlying principle between both physical rotated and phase delayed unit-cells is well detailed in [69]. The authors have presented a detailed comparison between both types of unit-cells through simulations and practical validation in two different transmitarray prototypes. Their study reveal that the transmitarray based on physically-rotated unit-cells exhibits wideband cross-polarisation filtering characteristics, whereas the one with phase-shifted cells can offer polarisation diversity (linear- and cross- polarisation) with similar performance to the former, but limited by 3 dB axial-ratio bandwidth and magnitude of the feeding antenna [69].

After analysing the presented examples, both loss and bandwidth may be considered the two major challenges in the design of a transmitarray. Hence, consideration to this aspect should be given at the time of selecting the design layout for a transmitarray implementation, given the project specifications. For example, in FSS-type transmitarray, bandwidth can be easily increased at the expense of using several stacked layers, as already mentioned. However, the overall insertion loss will always be proportional to the total number of layers (and on the properties of the substrate) and, thus, difficult to compensate. On the other hand, transmitarray with unit-cells composed of microstrip patches commonly exhibit limited bandwidth typically associated to such structures [1], but the insertion loss can be reduced by using amplifiers placed between the inner and the outer faces of the transmitarray. In fact, this technique has already been reported in [70–77], but particularly in [75], a total average gain of about 7.7 dB is reported for experiments on the unit-cell of Fig. 2.16, overcoming the initial insertion loss of 2.6 dB experienced without any signal amplification.

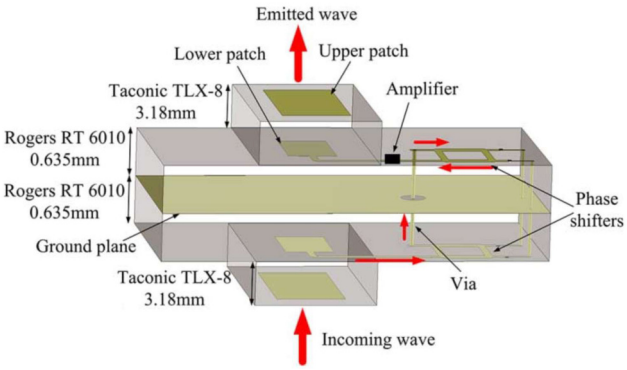

(a)

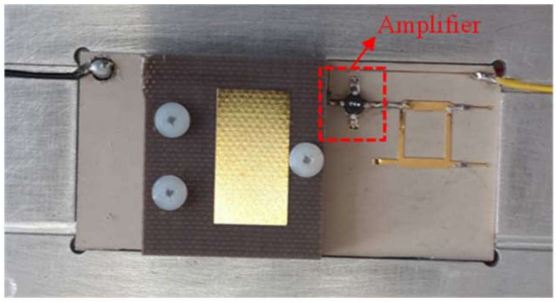

(b)

Figure 2.16: (a) Transmitarray unit-cell architecture and (b) photography of the unit-cell prototype (images extracted from the work presented in [75]).

2.4 HYBRID TRANSMITARRAY

Although the previous transmitarray designs [64–68] are not electronically reconfigurable (most are reconfigurable by mechanical rotation means), they yield to the development of hybrid reconfigurable transmitarray with both beamsteering and polarisation capabilities.

It is the case of the reconfigurable transmitarray presented in [78] by *Huang, C. et. al.*. The authors have developed a transmitarray operating at 5.4 GHz with the capability of controlling electronically the polarisation and direction of the re-radiated wave. Each unit-cell of the transmitarray is composed of several PCB layers separated by three different substrates, as depicted in Fig. 2.17. The face in which the electromagnetic wave is incident (Rx cell), a two-layer stacked patch is adopted. After being received by the Receiver (Rx) cell, the RF signal passes by two cascaded reflection type phase shifters and is coupled to the Transmitter cell (Transmitter (Tx) cell) through a metallized via hole. Each of the phase shifter implemented integrate a four-port directional coupler and each port is loaded by a varactor-based tunable circuit in order to achieve the 360° phase tuning range. The Tx cell is made of a square patch with an O-slot structure loaded with two p-i-n diodes inserted along the X and Y directions in order to control the polarisation of

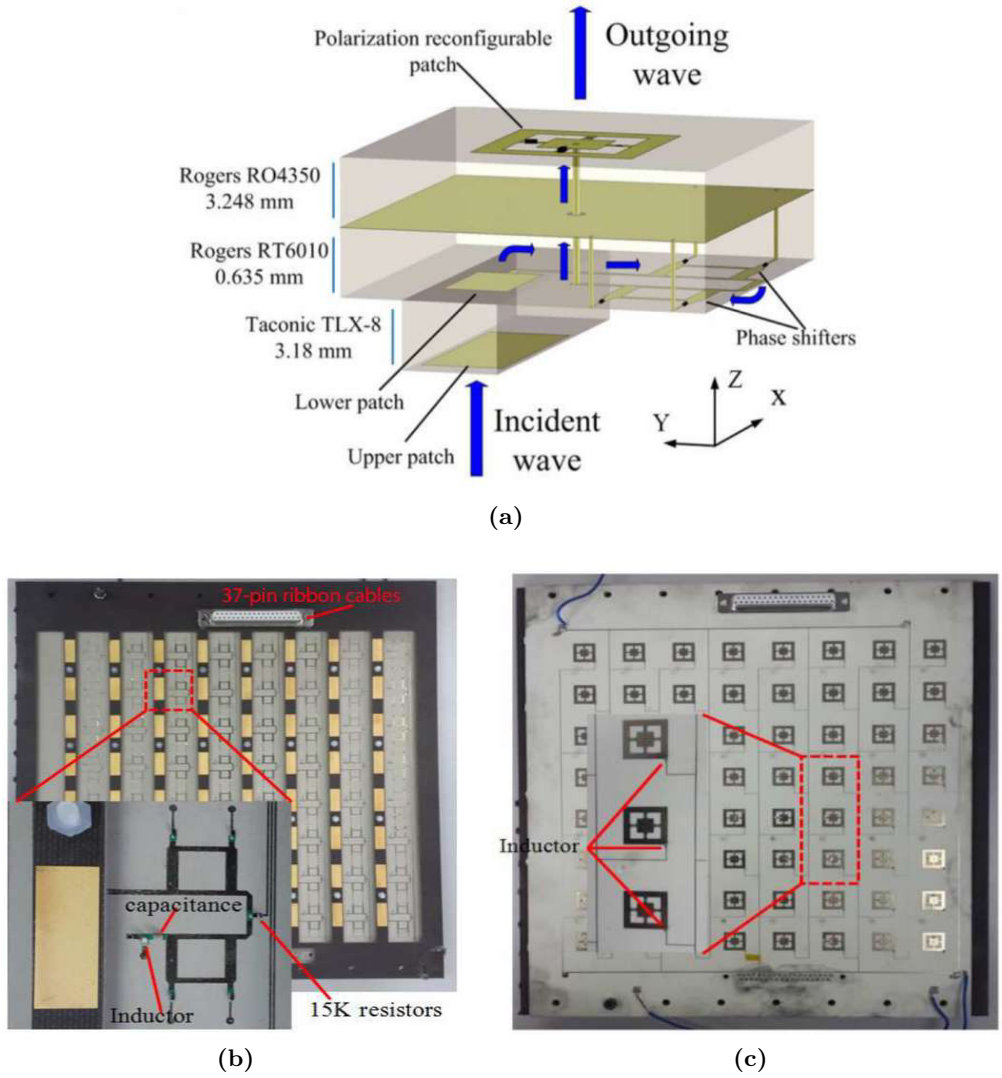

(a) **(b)** **(c)**

Figure 2.17: Transmitarray unit-cell architecture (image extracted from the work presented in [78]).

the outgoing wave. According to simulations, the insertion loss of the unit-cell varies between 1.5 and 5 dB at frequencies around 5.4 GHz, and a cross-polarisation ratio higher than 25 dB is obtained. The 8×8 transmitarray prototype is illustrated in Figs 2.17b and 2.17c. Experimental results demonstrate that this transmitarray is capable of achieving $\pm 6o°$ in both azimuth and elevation planes, having a difference of 3.8 dB between the gain of the broadside beam and at the scan angle of $6o°$. Experimental results also show that this transmitarray is capable of producing an outgoing wave with circular polarisation by controlling each of the p-i-n diodes independently.

In [79] yet another transmitarray with polarisation control capabilities is presented by the same authors of [78], based on the unit-cell of Fig. 2.18. The authors have suggested two designs of unit-cells for 1-bit phase resolution transmitarray, to operate around 10 GHz. The most complete design presented by the authors consists

of two-layer metallic patterns connected by a metallized via-hole as depicted in Fig. 2.18a. A U-slot rectangular patch is used in one side of the structure to receive the incident wave. On the other side, a square ring patch with two triangular corners and loaded with 2 p-i-n diodes is utilized to produce circular polarisation. The p-i-n diodes were used to dynamically select between LHCP and RHCP. The unit-cell operates under two cases: case 1 - p-i-n diode 1 is switched ON while 2 is OFF; case 2 - p-i-n diode 1 is switched OFF while 2 is ON. Simulated results (Fig. 2.18b, Fig. 2.18c) on the unit-cell were further validated on a 8×8 transmitarray prototype against experimental results (Fig. 2.18d, Fig. 2.18e). While in case 1, the transmitarray converts a vertically polarised incident wave to RHCP, in case 2 the transmission phase of the outgoing wave is also shifted by 180°. Based on the previous unit-cell design [79], the same research group have introduced and characterized in [80], a transmitarray with both reconfigurable polarisation control and beamsteering capabilities. Besides of controlling the polarisation of the re-transmitted EM wave, the proposed transmitarray also has the capability of realising beamsteering in a range of $\pm 45°$ in both elevation an azimuth planes at 4.8 GHz, exhibiting however insertion losses of 5.6 dB over a small bandwidth of 100 MHz, obtained experimentally on a manufactured prototype.

Similarly in [81], it has been presented a 20×20 element fully reconfigurable transmitarray based on a 1-bit linear polarisation unit-cell model operating in the Ka-band (27-GHz). A snapshot of both unit-cells and the reconfigurable transmitarray are depicted in Fig. 2.19. The unit-cell is formed in a multi-layer design with a central ground plane (Fig. 2.19a) loaded with p-i-n diodes to obtain a wide-band constant phase shift between the two phase states. Circular polarisation is achieved by using the sequential rotation technique previously described, while p-i-n diodes enable LHCP / RHCP polarisation switching. However, due to the control of the phase shift by switching on and off the p-i-n diodes, the control of the direction of the out-coming wave is also possible with reported steering ranges of $\pm 60°$ in azimuth and elevation planes.

Finally, in [82] a 1-bit reconfigurable transmitarray that allows control of polarisation as well as antenna beamsteering is presented. The unit-cell of the transmitarray is comprised of two H-shaped slots (Fig. 2.20a) that behave as receiving and transmitting coupled microstrip patches. The fact that they are orthogonality disposed relative to each other, it allows X to Y polarisation transformation (of the incident EM wave). In between the transmitter and receiver slot patches, a feeding network that includes 2 p-i-n diodes is responsible to control the phase difference of the arrangement. When the p-i-n diode 1 is OFF and p-i-n diode 2 is ON (Fig. 2.20a), a total phase shift of 180° is achieved against 0° phase shift for the opposite case. The proposed unit-cell operates at a center frequency of 12.5 GHz and it has an overall dimension of $8 \times 8\ mm^2$ ($\lambda/3 \times \lambda/3$). According to simulation on the unit-cell, the

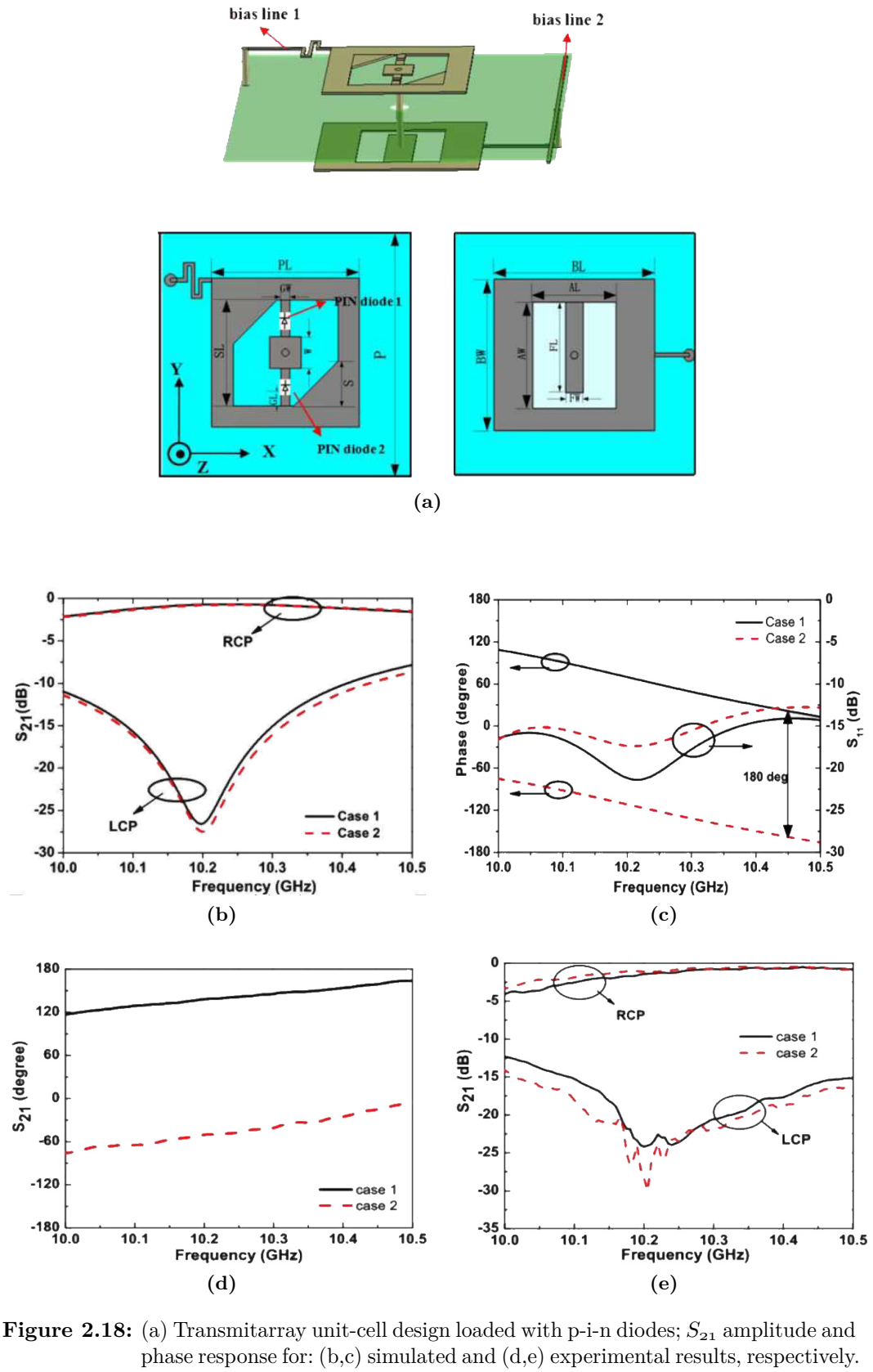

Figure 2.18: (a) Transmitarray unit-cell design loaded with p-i-n diodes; S_{21} amplitude and phase response for: (b,c) simulated and (d,e) experimental results, respectively. (images extracted from the work presented in [79]).

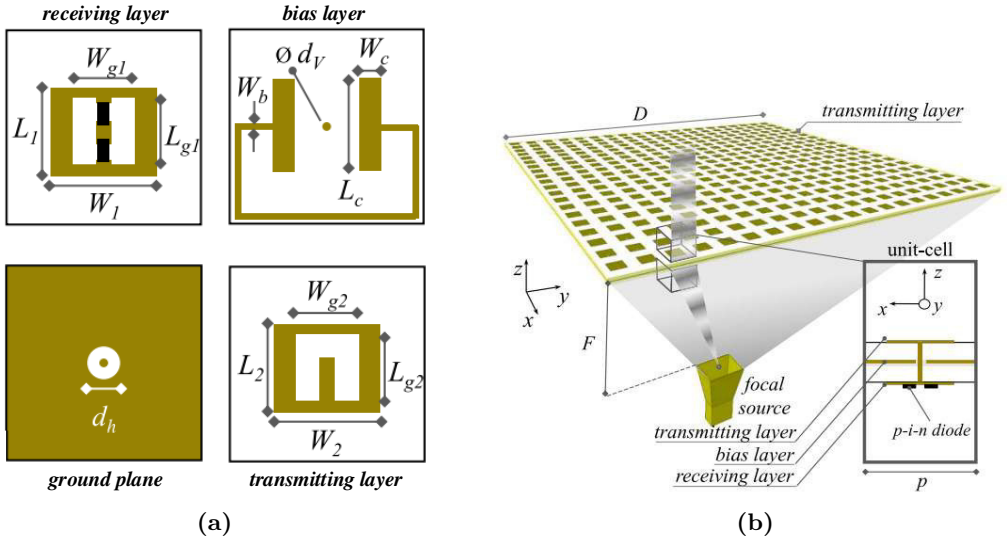

Figure 2.19: Snapshot of (a) the active unit-cell and (b) transmitarray for beamsteering and polarisation control (images extracted from the work presented in [81]).

-10 dB S_{11} bandwidth is of 300 MHz for both working cases, with maximum of 0.86 dB of insertion losses (for the case where D1=OFF/D2=ON). The isolation between co- and cross-polarisations is 16.5 dB for the center frequency.

Subsequent to the unit-cell characterization, a 16×16 transmitarray prototype has been fabricated and measured. It is composed of 256 individual cells leading to a total of 512 p-i-n diodes to achieve both phase and angular reconfigurability. A *x-polarised* horn feed is used to illuminate the transmitarray as shown in Fig. 2.20b. With the presented setup, a total of $\pm 50^\circ$ beamsteering is obtained for both elevation and azimuth planes.

It should be noted that some authors consider that the transmitarray are placed at a distance far away from the radiation source aperture (focal distance), whereas others are considered at the vicinity of the antenna source aperture. The ones that are placed at the right focal distance typically exhibit wide beamsteering ranges, since the placement at the focal distance leads to better spillover and illumination efficiencies.

In fact, this is well reported in [83] where the authors have developed a flat lens exhibiting circular polarisation and wide beamsteering angular ranges (Fig. 2.21). In particular, the focal seems to play distance play an important role in radiation performance, since larger distances tend to reduce aberration and consequently lower beam distortions and improve side-lobe levels. To this end, the authors in [83] have proposed a new feeding technique by implementing a virtual focus using a dual-lens configuration, in order to reduce the overall antenna height. Remarkably, beamsteering angles up to $\pm 50^\circ$, at Ka-band (30 GHz) with an antenna height estimated to be reduced by 20%, due to the virtual focus, has been achieved. In

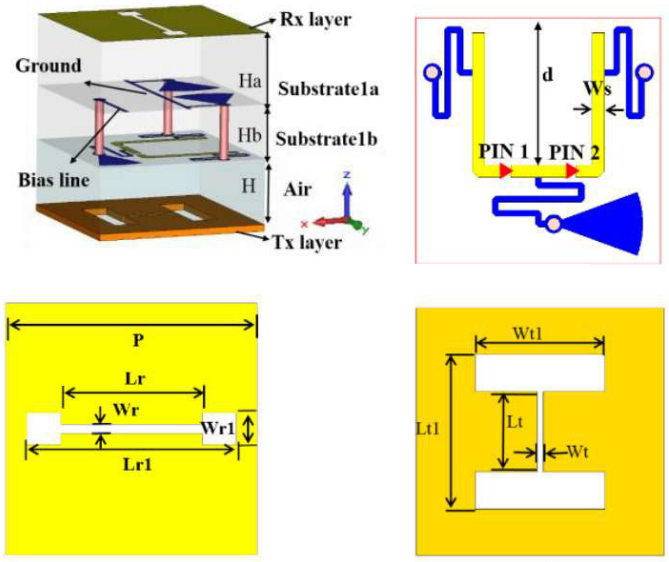

(a)

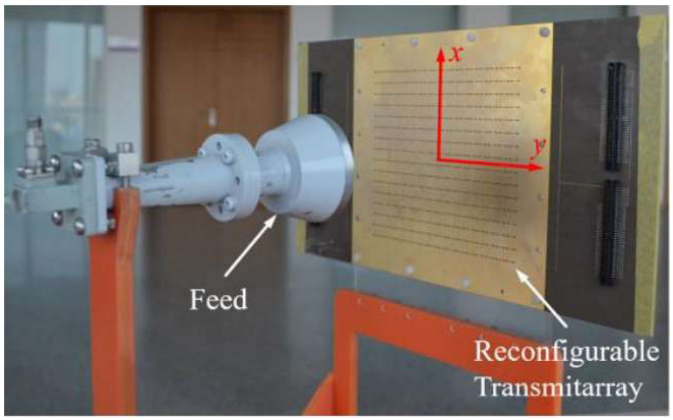

(b)

Figure 2.20: (a) Geometry of the transmitarray element and (b) reconfigurable transmitarray prototype with 16×16 elements (images extracted from the work presented in [82]).

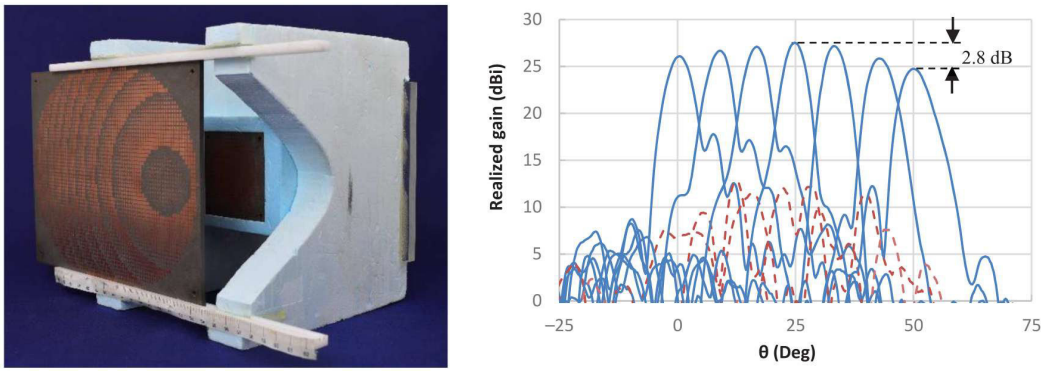

(a) (b)

Figure 2.21: (a) Antenna prototype and (b) measured realized gain for several beamsteering angles between 0° and 50° (images extracted from the work presented in [83]).

fact, this is different technique to those previously presented, in which a lens-like phase pattern, by means of microstrip patches, is used for beamsteering.

The closer the feed, the higher the oblique incident angle, which in turn affects negatively the illumination efficiency and thus overall steering ranges. However, the transmitarray placed right next to antenna aperture also showed to processing results with the advantage of reducing the overall size of the apparatus.

The references presented in this review of the literature are summarized in Table 2.1, listed by their main feature (polarisation control and beamsteering), mode of operation (P - passive, A - active), Unit-cell (UC) design format and size, reconfigurability control mechanism, frequency of operation, bandwidth, insertion losses and beamsteering angular ranges with respective steering planes, when applicable.

Table 2.1: Summary table of references for polarisation control (Pol.) and beamsteering (BS) transmitarrays

Ref.	Feature	Mode†	UC type	UC size	Control mechanism	Freq. band	Bandwidth	Loss	BS Range
[39]	BS	A	microstrip patch	n/a	varactor	12 GHz	700 MHz	3 dB	$9°Az\ only$
[40, 41]		A	microstrip patch	$0.55\lambda \times 0.55\lambda$	varactor	5.7 GHz	n/a	4.8dB	$\pm 25°{}^{\star} Az\ or\ El$
[42]		A	coupled feed patch	$0.55\lambda \times 0.55\lambda^{*}$	varactor	5 GHz*	500 MHz*	3.6 dB*	n/a
[43]		A	coupled feed patch	$0.55\lambda \times 0.55\lambda$	varactor	5 GHz	500 MHz	2.2 dB	$\pm 50°{}^{\star} Az\ and\ El$
[44–46]		A	microstrip patch	$0.5\lambda \times 0.5\lambda$	p-i-n (and MEMS)	10 GHz	1.5 GHz	3 dB	$\pm 70° Az\ and\ \pm 40° El$
[47]		A	O-slot rectangular patch	$\lambda/2 \times \lambda/2$	p-i-n	29 GHz	n/a	n/a	$\pm 40°{}^{\star} Az\ only$
[48]		A	microstrip patch	n/a	varactor diodes	24.6 GHz	1 GHz	17 dB	$\pm 50° Az\ and\ El$
[16]		A	metamaterials	n/a	liquid crystal	27.5 GHz	n/a	5 dB	$\pm 5° Az\ only$
[49]		A	metamaterials	$0.17\lambda \times 0.17\lambda$	varactor	1.7 GHz	n/a	4 dB	$\pm 30°{}^{\star} Az\ only$
[50]		A	metamaterials	$0.61\lambda \times 0.61\lambda$	varactor	4.7 GHz	250 MHz	n/a	$\pm 30°{}^{\star} Az\ only$
[52–54]		A	freq. selective surface	$0.5\lambda \times 0.5\lambda^{*}$	varactor	4 GHz*	400 MHz*	3 dB*	n/a
[55]		A	freq. selective surface	$0.58\lambda \times 0.58\lambda$	varactor	5.3 GHz	180 MHz	6.5 dB	$\pm 30°{}^{\star} Az\ or\ El$
[56]		A	freq. selective surface	$\lambda/25 \times \lambda/25$	tunable ferroelectric film	12 GHz	n/a	2.9 dB	$\pm 10° Az\ only$
[57]		P	freq. selective surface	$0.17\lambda \times 0.17\lambda$	discrete capacitors	5.35 GHz	110 MHz	2.8 dB	$\pm 25° Az\ and\ El$
[58]		A	freq. selective surface	$0.17\lambda \times 0.17\lambda$	varactor	5.2 GHz	70 MHz	4.3 dB	$\pm 28° Az\ and\ \pm 26° El$
[59]		A	freq. selective surface	$0.54\lambda \times 0.54\lambda$	p-i-n	11.5 GHz	n/a	n/a	$\pm 40° Az\ and\ El$
[64, 65]	Pol	P	microstrip patch	$0.5\lambda \times 0.5\lambda^{*}$	cell rotation	60 GHz*	5.6 GHz*	0.46 dB*	n/a
[66]		P	microstrip patch	$0.5\lambda \times 0.5\lambda$	cell rotation	30 GHz	6.5 GHz	n/a	n/a
[67]		P	multi-layer PCB	$0.28\lambda \times 0.28\lambda$	cascading surfaces	77 GHz	13 GHz	n/a	n/a
[68]		P	cascaded rectangle ring slot	$0.6\lambda \times 0.6\lambda$	feeding source rotation	6 GHz	1.8 GHz	n/a	n/a
[78]	Hybrid (BS & Pol)	A	square patch	$0.482\lambda \times 0.482\lambda$	varactor (and p-i-n)	5.4 GHz	450 MHz	3.8 dB	$\pm 60° Az\ and\ El$
[79]		A	U-slot patch	$0.47\lambda \times 0.47\lambda$	p-i-n	10 GHz	320 MHz	1.4 dB	n/a
[80]		A	U-slot coupled feed patch	$0.488\lambda \times 0.488\lambda$	p-i-n	4.8 GHz	100 MHz	5.6 dB	$\pm 45° Az\ and\ El$
[81]		A	rectangle ring slot	$0.46\lambda \times 0.46\lambda$	p-i-n	27 GHz	4.2 GHz	3 dB	$\pm 60° Az\ and\ El$
[82]		A	U-shaped microstrip line	$\lambda/3 \times \lambda/3$	p-i-n	12.5 GHz	300 MHz	5 dB	$\pm 50° Az\ and\ El$
[83]		P	dual layer microstrip patch	$\lambda/3 \times \lambda/3$	n/a	30 GHz	2 GHz	n/a	$\pm 50° El$

† modes for unit-cells: P - passive, A - active (reconfigurable);
* considering the best case of 2 proposed designs;
⋆ steering range with SLL<12dB;
n/a - not available.

2.5 INTERIM CONCLUSIONS

This chapter presents an extensive literature review addressing antenna beamsteering by using transmitarray. The literature review is outlined starting with transmitarray developed for antenna beamsteering, wavefront polarisation control, and transmitarray that combine both features simultaneously. Particular emphasis is given to active/reconfigurable transmitarray, i.e. devices with the capability of having its characteristics electronically controlled, either by employing active mechanisms as p-i-n diodes, varactor diodes or MEMS switches. Several examples among the literature have been presented and compared, followed by a critical review. Information about unit-cell main characteristics are disseminated including, design layout, e.g. if based on FSS, MM or microstrip patch antennas. Finally, all this information is summarized in terms of useful technical data extracted from the literature such as, frequency of operation, bandwidth, unit/cell dimensions, insertion loss and maximum steering ranges. This review demonstrates that transmitarray antennas can be seen as a feasible alternative to the most traditional techniques of beamsteering, overcoming some of its limitations, e.g. it withdraws the requirements of complex beamsteering networks of phased antenna arrays. Since transmitarray are mostly employing using PCB techniques, they will significantly reduce weight, power consumption and the dimensions of assemblies, making them very attractive for inclusion in a large number of applications that goes beyond antenna beamsteering, as the candidate has demonstrated in a work developed prior to this dissertation, and published in [63].

This page is intentionally left blank.

3

BEAMSTEERING WITH A TRANSMITARRAY

3.1 INTRODUCTION

This chapter introduces the theoretical background for antenna beamsteering using a transmitarray. In particular, the mode of operation of a conventional 1D beamsteering transmitarray is described and compared against a typical linear antenna array. Additionally, a theoretical approach to perform 2D beamsteering using a transmitarray is presented.

3.2 THEORETICAL MODEL FOR 1D–BEAMSTEERING

The principle of beamsteering using a traditional transmitarray can be compared to the one using a linear antenna array. Figure 3.1 depicts both configurations for comparison. In a linear antenna array, the phase shifting is applied to the signal in each individual branch using a phase shifter [1–3], whilst in a transmitarray the phase shifting is obtained by controlling the phase delay introduced by each individual elements of the transmitarray, as reported in [13–15, 39–50, 52–59].

When an incident EM wave propagates through a transmitarray of length l, composed by N elements of periodicity p (Fig. 3.1b), it experiences a different phase

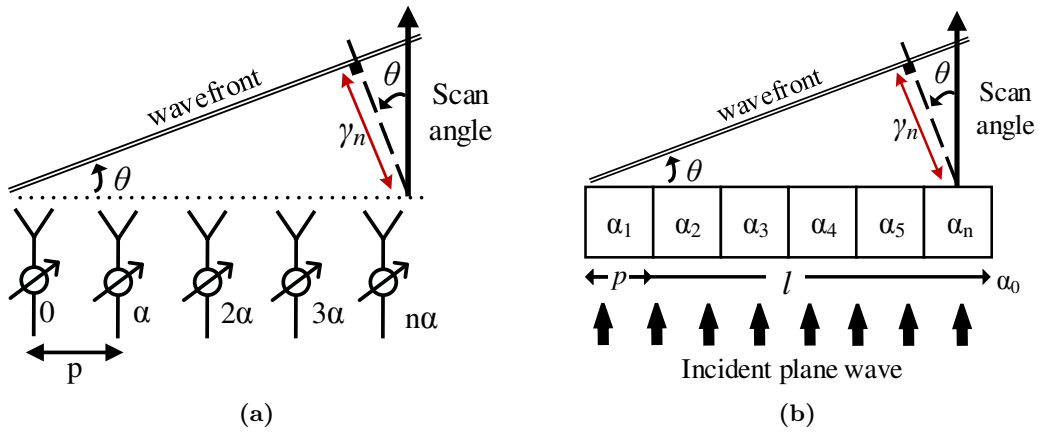

Figure 3.1: (a) Model of linear antenna array and (b) model of a transmitarray for 1D beamsteering analysis.

shifting γ_n expressed by (3.1), after penetrating each of the elements of the array in the steering direction theta θ,

$$\gamma_n = \frac{2\pi}{\lambda_0}.p.n.sin(\theta) = k_0.p.n.sin(\theta), \tag{3.1}$$

where $k_0 = \frac{2\pi}{\lambda_0}$ is the wave number in free space.

Consequently, the transmission phase α_n in the n^{th} element, can be defined by (3.2),

$$\alpha_n = -\gamma_n + \alpha_0 + 2\pi i, \qquad i \;\; 0,1,2,... \tag{3.2}$$

where α_0 is the phase of the incident EM wave at the input of the transmitarray.

Therefore, the re-transmitted wave direction θ can be expressed as a function of the phase difference ψ between adjacent elements, *i.e.* progressive phase, using (3.3),

$$\begin{aligned} \psi = \alpha_n - \alpha_{n-1} = -\gamma_n + \gamma_{n-1} = \\ = -k_0.p.n.sin(\theta) + k_0.p.(\text{n-1}).sin(\theta) = -k_0.p.sin(\theta). \end{aligned} \tag{3.3}$$

Thus, by varying the phase α_n of each array element in a progressive way, the incident wave can be steered to a desired direction θ relative to the normal of the structure, defined by (3.4),

$$\psi = -k_0.p.sin(\theta) \Leftrightarrow \theta = -sin^{-1}\left(\psi.\frac{\lambda}{2\pi.p}\right) \tag{3.4}$$

However, since the phase distribution in the array is applied along a single direction only, the model for a linear transmitarray limits its application to 1D beamsteering. Therefore, the main lobe of the radiation pattern of the original antenna in which the transmitarray is applied, only has the capability to be steered towards the output angle with θ component, as reported in some of the references included in the literature review [16, 39–41, 49, 50, 55, 56].

3.3 THEORETICAL MODEL FOR 2D–BEAMSTEERING

In order to extend the concept to 2D beamsteering using a transmitarray, it is proposed herein to characterise the model by analogy with a planar antenna array. This vision, proposed in the work of [5], enables the transmitarray to have the control over the two angular components theta θ and phi ϕ of the output angle direction, simultaneously, raising the limitation of 1D beamsteering of the previous model. The transmitarray model for 2D beamsteering is depicted in Fig. 3.2.

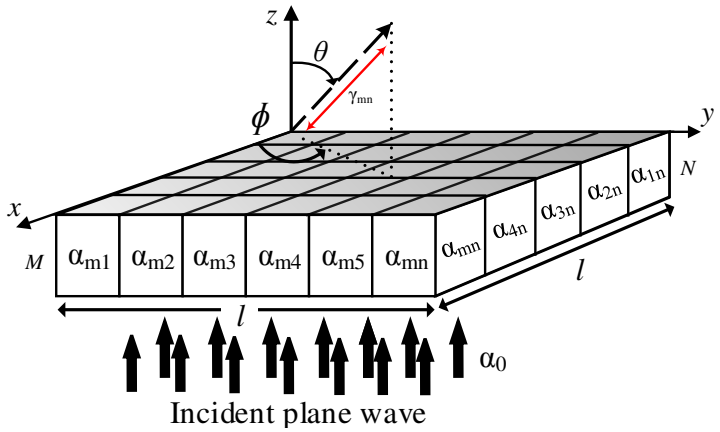

Figure 3.2: Proposed model for a transmitarray with 2D beamsteering.

Built on the theory of planar antenna arrays, presented in [1] and [3], a progressive phase shift between adjacent elements should occur along the X and Y directions of the $M \times N$ array so 2D beamsteering could be enabled. Thus, by expanding from (3.3), the relation between the two dimensional output directions (θ,ϕ) and the progressive phase delay, is given by (3.5),

$$\begin{cases} \psi_x = -k_0.p.sin(\theta).cos(\phi) \\ \\ \psi_y = -k_0.p.sin(\theta).sin(\phi) \end{cases}, \tag{3.5}$$

where ψ_x and ψ_y are the progressive phase along X and Y axis, respectively, and p is the periodicity of the $p \times p$ array elements.

Therefore, a $M \times N$ transmitarray would exhibit a relative phase distribution that can be represented by the matrix (3.6),

$$\begin{array}{c} \\ \psi_y \downarrow \end{array} \begin{array}{c} \rightarrow \psi_x \\ \begin{bmatrix} \alpha_{1,1} & .. & .. & .. & .. & \alpha_{1,n} \\ .. & .. & .. & .. & .. & .. \\ .. & .. & .. & .. & .. & .. \\ \alpha_{m,1} & .. & .. & .. & .. & \alpha_{m,n} \end{bmatrix} \end{array} \tag{3.6}$$

where $\alpha_{m,n}$ is the phase delay introduced by each individual (m,n) element of the transmitarray. This representation is proposed herein to facilitate the understanding of the progressive phase along the transmitarray and will be further considered hereafter.

From this analysis, it can be concluded that the output steering direction (θ,ϕ) depends on the transmission phase $\alpha_{m,n}$ of each element of the 2D transmitarray,

and similarly to (3.2) (linear case), the phase shifting in each individual element can be described by (3.7),

$$\alpha_{m,n} = -\gamma_{m,n} + \alpha_0 + 2\pi i, \qquad i = 0,1,2,... \tag{3.7}$$

where the phase shifting of each element $\alpha_{m,n}$ is a periodic function, and $\alpha_{m,n} \subset 0,2\pi$ such as in the 1D case. Thus, each element of the transmitarray must always be capable to achieve at least 360° (2π) of transmission phase shift, to ensure a complete control of the output angle.

Notwithstanding, in order to directly match the output angle direction obtained from the theory with the output angle direction given either by simulation and experiments, it is proposed, by this work, to apply in the theoretical model a coordinate system conversion from Spherical coordinates (represented by θ and ϕ components) to *Azimuth-over-Elevation* (represented by the pair *Az/El*). Therefore, the mathematical relation between spherical and *Az/El* coordinates well detailed in [84], given by (3.8), has been applied here:

$$\begin{cases} sin(\theta).cos(\phi) = cos(El).sin(Az) \\ \\ sin(\theta).sin(\phi) = sin(El) \end{cases} . \tag{3.8}$$

The main differences between both coordinate systems rely on the origin of the axis, as depicted in Fig. 3.3. From the mathematical workout resultant of replacing (3.8) in (3.5), a generic formula to calculate the output angle direction with *Az/El* components provided by a 2D transmitarray, is given by (3.9),

$$\begin{cases} \psi'_x = -k_0.p.cos(El).sin(Az) \\ \\ \psi'_y = -k_0.p.sin(El) \end{cases} . \tag{3.9}$$

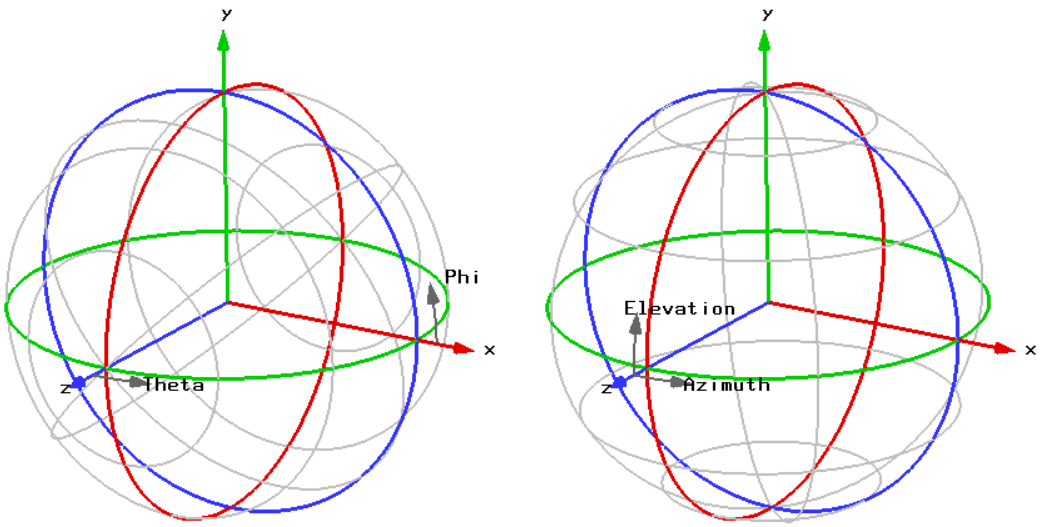

(a) **(b)**

Figure 3.3: Axial representation of the (a) spherical coordinate system (θ/ϕ) and (b) *Azimuth-over-Elevation* coordinate system Az,El.

3.4 INTERIM CONCLUSIONS

This chapter introduces the theoretical background for antenna beamsteering using a transmitarray. After presenting the theoretical model for 1D beamsteering using a transmitarray, an approach for the analysis of a transmitarray with 2D beamsteering has been introduced. With this, it was verified that to perform beamsteering with a transmitarray, the phase in each transmitarray element must be varied, progressively and equally, throughout the entire array much like a phased antenna array.

This page is intentionally left blank.

4

DESIGN OF A PASSIVE TRANSMITARRAY

4.1 INTRODUCTION

In this chapter, a transmitarray with two-dimensional beamsteering capabilities inspired on FSS is presented, at frequencies of 28 GHz. Following the requirements of the theoretical model introduced in the last chapter, a controlled phase shift is applied to each transmitarray element in order to enable the steering of the main lobe of an original antenna pattern, in both elevation and azimuth planes. This is accomplished by introducing a stacked, square-slot, unit-cell structure with band-pass filtering characteristics controlled via Surface Mount Devices (SMD) capacitors loaded into the cell. This was finally verified in a 5x5 transmitarray composed of such unit-cells.

A complete parametric study based on electromagnetic simulations using CST MWS is presented to evaluate and characterize the unit-cell parameters. In particular, the phase characterization in terms of its variation and response with layer stacking, distance separation and substrate thickness is studied. Antenna beamsteering with ranges of up to $\pm 28^{\circ}$ in both azimuth and elevation are achieved by means of EM simulations at 28 GHz, using the 5×5 array configuration. An output angle compensation model is also presented to correct the steering angle and decrease the steering error.

4.2 STACKED UNIT CELL

The unit-cell design proposed herein is depicted in Fig. 4.1a. It follows the square-slot FSS design presented in [58]. For the operation frequency of 28 GHz, the cell dimensions are detailed in Table 4.1. Each unit cell is loaded with two discrete capacitors in order to control the phase shift introduced in the incident wave.

The respective equivalent circuit is presented in Fig. 4.1b, where L represents the inductance of the outer loop, C_g the parasitic capacitance introduced by the gap of the slot and C_d the capacitance of the SMD capacitors. The first two parameters are specified by the dimensions of the FSS, the latter being the one that can be controlled to achieve the desired output angle. A Nelco NX9250 substrate with a

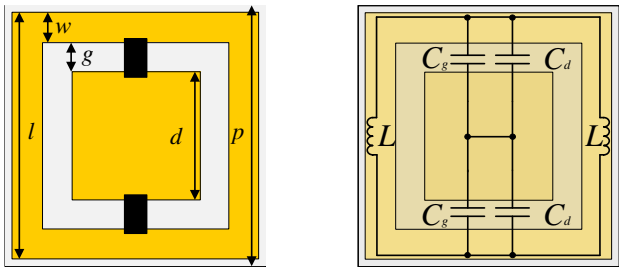

(a) (b)

Figure 4.1: (a) Square slot FSS unit cell and (b) unit cells equivalent circuit.

Table 4.1: Unit cell dimensions

Parameter	Value (mm)
p	5.75
l	5.55
d	4.06
g	0.34
w	0.41

relative permittivity (ϵ_r) of 2.5 and a dissipation factor ($\tan\delta$) of 0.0017, has been considered for the simulations.

This unit-cell acts as a bandpass filter, in which the pass band response is controlled by the dimensions of the cell but also by the SMD capacitors value according to (4.1).

$$f_c = \frac{1}{\pi \times \sqrt{L \times (C_g + C_d)}} \tag{4.1}$$

As previously stated, when an incident wave propagates through the FSS, it undergoes a phase shift depending on the SMD capacitor introduced. However, in order to achieve the total phase shift necessary to fully control the beamsteering, one layer of FSS is not sufficient due to the low phase shifting associated to a single layer, as reported in [57] and, according to literature, at least 360° are needed.

To this end, a parametric study in CST MWS was performed to evaluate the optimal number of layers, substrate thickness and distance between layers required to achieve the necessary phase shift to enable beamsteering. The results of this parametric study are presented in Tables 4.2, 4.3 and 4.4 for substrates of thickness 0.254, 0.635 and 0.762 mm, respectively. These dimensions were selected to match the standard substrates thickness available in the market. In this parametric study, the effect of varying the number of layers (between 1 and 7) and the distance between them (between 0.5 and 2 mm) in the unit-cell were studied in terms of centre frequency (f_c), bandwidth, maximum phase shift ($\Delta\alpha$) and insertion losses (I_{loss}).

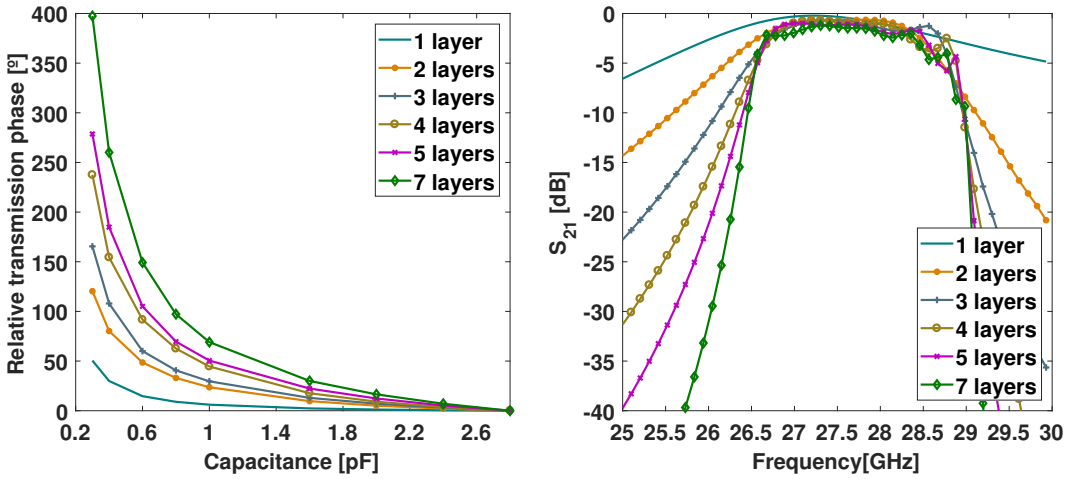

(a) (b)

Figure 4.2: Dependency of (a) total phase shift and (b) S_{21} with the variation of number of layers for 1pF, considering Case 1.

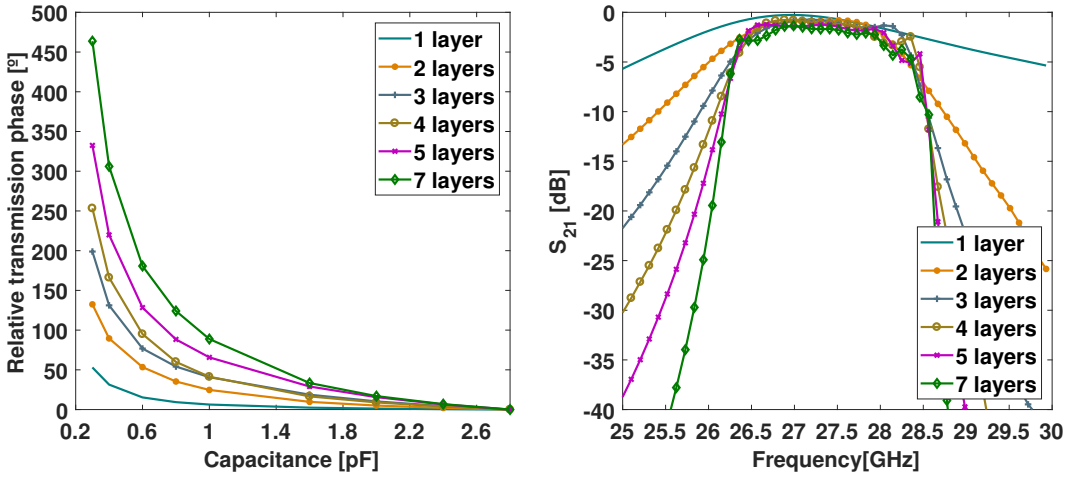

(a) (b)

Figure 4.3: Dependency of (a) total phase shift and (b) S_{21} with the variation of number of layers for 1pF, considering Case 2.

The bandwidth of the unit-cell is defined by the frequency difference between the higher -3 dB point of the maximum capacitance value (2.8 pF) and the lower -3 dB point of the minimum capacitance value (0.3 pF). Furthermore, for all parametric combinations, it is characterised I_{loss} as the maximum value of insertion losses within the pass band, which in some cases are higher than -3 dB due to the oscillation in the pass band. All these values can be calculated through the S_{21} parameter of the unit-cell. The S-parameters describe the input-output relationships between ports in an electrical system. For a device with two ports there are four S-parameters: S_{11} and S_{22} which are the direct and inverse voltage reflection coefficients, respectively and S_{21} and S_{12} which are the direct and inverse voltage transmission coefficients, respectively [85].

Table 4.2: Parametric study on number and distance between layers for a substrate with thickness 0.254 mm.

Distance between layers (mm)	**Number of layers**	f_c **(GHz)**	**BW (GHz) / (% of f_c)**	$\Delta\alpha(^\circ)$	$\mathbf{I_{loss}}$ **(dB)**
	1	28.1275	1.682 / 5.98	42	1.02
	2	28.2305	1.51 / 5.35	68	0.6
	3	28.3755	1.751 / 6.17	100	3.16
0.5	4	28.2385	1.361 / 4.82	122	1.67
	5	28.3475	1.61 / 5.68	159	1.21
	7	28.0945	1.179 / 4.2	210	1.7
	2	28.3285	1.332 / 4.7	78	0.4
	3	28.583	1.578 / 5.52	103	3
0.7	4	28.3705	1.087 / 3.83	140	1.39
	5	28.5105	1.359 / 4.77	178	0.84
	7	28.4495	1.272 / 4.47	252	3.6
	2	28.2935	1.03 / 3.64	92	0.6
	3	28.5525	1.271 / 4.45	113	2.35
1	4	28.3315	0.733 / 2.59	177	0.9
	5	28.464	0.998 / 3.51	201	2.62
	7	28.3925	0.913 / 3.22	293	2.94
	2	28.1285	0.658 / 2.34	110	1.26
	3	28.318	0.848 / 2.99	146	1.26
1.5	4	28.3995	0.997 / 3.51	192	3.31
	5	28.19	0.628 / 2.23	261	1.58
	7	28.1275	0.562 / 2	382	3.14
	2	27.9695	0.457 / 1.63	122	1.8
	3	28.0645	0.561 / 2	181	0.84
2	4	28.112	0.736 / 2.62	224	2.1
	5	28.1375	0.845 / 3	291	3.7
	7	28.0905	0.533 / 1.9	400	2.71

Table 4.3: Parametric study on number and distance between layers for a substrate with thickness 0.635 mm.

Distance between layers (mm)	**Number of layers**	f_c **(GHz)**	**BW (GHz) / (% of f_c)**	$\Delta\alpha(^\circ)$	$\mathbf{I_{loss}}$ **(dB)**
	1	28.1545	1.343 / 4.77	50	1.4
	2	28.0875	0.575 / 2.05	120	1.61
	3	28.2315	0.681 / 2.41	165	1.75
0.5	4	28.0795	0.388 / 1.38	238	1.86
	5	28.1315	0.551 / 1.96	279	2.21
	7	28.0655	0.504 / 1.8	397	3.34
	2	28.1875	0.512 / 1.82	126	1.6
	3	28.3835	0.663 / 2.34	173	1.81
0.7	4	28.199	0.3 / 1.06	251	2.24
	5	28.2835	0.474 / 1.68	293	2.26
	7	28.2075	0.41 / 1.45	424	3.12
	2	28.1645	0.382 / 1.36	132	1.94
	3	28.343	0.568 / 2	184	1.44
1	4	28.4205	0.709 / 2.49	230	3.56
	5	28.2245	0.358 / 1.27	325	1.76
	7	28.173	0.29 / 1.03	467	3.66
	2	28.023	0.222 / 0.79	143	2.53
	3	28.1145	0.351 / 1.25	217	1.41
1.5	4	28.162	0.51 / 1.81	265	2.35
	5	28.1885	0.624 / 2.21	336	3.903
	7	28.142	0.302 / 1.07	483	3.14
	2	27.885	0.136 / 0.49	152	2.82
	3	27.887	0.209 / 0.75	244	2.02
2	4	27.908	0.356 / 1.28	306	2
	5	27.927	0.447 / 1.6	378	3.47
	7	27.8925	0.159 / 0.57	556	2.87

Table 4.4: Parametric study on number and distance between layers for a substrate with thickness 0.762 mm.

Distance between layers (mm)	**Number of layers**	f_c **(GHz)**	**BW (GHz) / (% of** f_c**)**	$\Delta\alpha(^\circ)$	$\mathbf{I_{loss}}$ **(dB)**
	1	27.923	1.3 / 4.66	53	1.61
	2	27.8	0.364 / 1.31	133	2.44
	3	27.917	0.418 / 1.50	199	1.56
0.5	4	27.957	0.541 / 1.94	253	3.5
	5	27.807	0.337 / 1.21	333	1.93
	7	27.8755	0.558 / 2.00	463	4.45
	2	27.89	0.307 / 1.10	138	2.26
	3	28.049	0.451 / 1.61	199	1.53
0.7	4	28.116	0.58 / 2.06	250	3.67
	5	27.956	0.313 / 1.12	338	1.86
	7	27.885	0.216 / 0.78	480	3.59
	2	27.868	0.231 / 0.83	143	2.5
	3	28.013	0.38 / 1.36	211	1.37
1	4	28.074	0.533 / 1.90	257	3.19
	5	27.894	0.223 / 0.80	355	2.25
	7	28.041	0.381 / 1.36	510	4.03
	2	27.729	0.116 / 0.42	155	2.93
	3	27.789	0.222 / 0.80	240	1.95
1.5	4	27.824	0.39 / 1.40	294	2.08
	5	27.847	0.45 / 1.62	360	3.58
	7	27.808	0.187 / 0.67	540	2.811
	2	27.59	0.059 / 0.21	163	3.12
	3	27.57	0.126 / 0.46	234	2.56
2	4	27.582	0.259 / 0.94	283	2.32
	5	27.603	0.346 / 1.25	390	3.9
	7	n/a	n/a	n/a	n/a

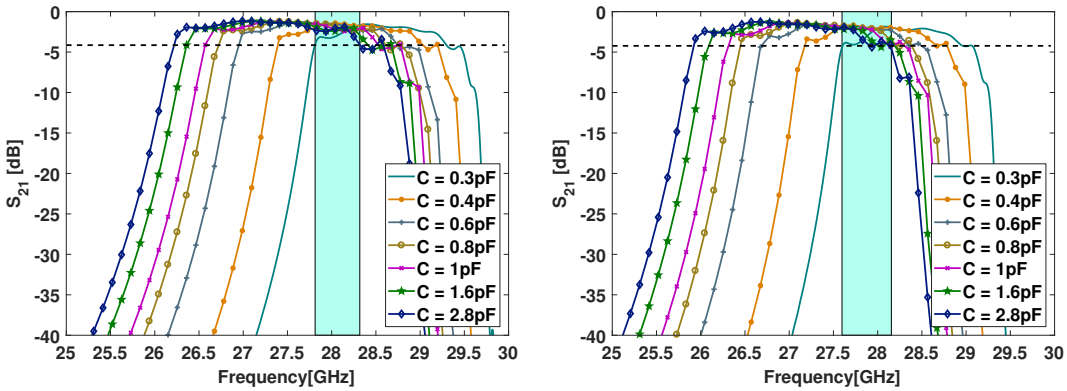

Figure 4.4: Dependency of S_{21} with value of capacitance for unit-stacked cell with 7 layers, considering (a) Case 1 and (b) Case 2.

Even though it is possible to attain the necessary phase shift with a 0.254 mm substrate, this results will not be considered for further analysis, since the substrate is very thin. When looking at implementation phase, a thicker substrate will be less prone to bending and other implementation problems, in which the ones with 0.635 and 0.762 mm should be considered for further simulations and transmitarray implementation. These results are presented to demonstrate that it is possible to obtain the same results for a variety of substrates using the correct parameters (in this case number of layers and distance between them).

Through the detailed analysis of the tables, it is possible to conclude that, in order to obtain the 360° of phase shift with 500 MHz of bandwidth, 7 layers with a distance of 0.5 mm between them are thus necessary, when considering a substrate with either 0.635 or 0.762 mm. This means that any of these substrates can be used in the transmitarray. For the characterisation, two-case studies have been considered: Case 1 - 0.635 mm; and Case 2 - 0.762 mm.

According to the results presented in Tables 4.2, 4.3 and 4.4, Fig. 4.2a depicts the total transmission phase achieved for the different number of layers, for a range of capacitance values between 0.3 and 2.8 pF, considering Case 1. Fig. 4.2b shows how the number of layers influence the S_{21} of the stacked unit-cell when considering the same value of capacitance introduced in the gap (in this case 1 pF). Similar results for Case 2 are presented in Fig. 4.3.

Subsequently, the S_{21} parameters for 7 layers depending on the capacitance values are presented in Fig. 4.4 for both cases, where the considered operating bands are shown. In these plots, it is possible to better understand how the bandwidth of each unit-cell is calculated.

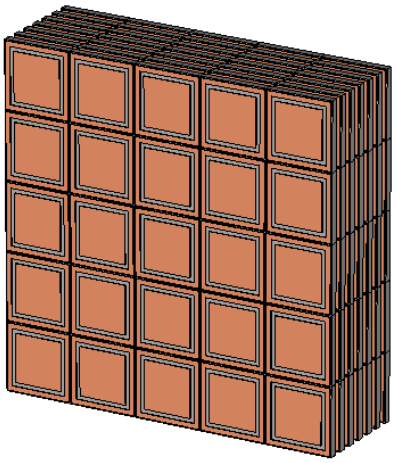

Figure 4.5: 5x5x7 full transmitarray.

4.3 FULL STRUCTURE SIMULATION AND BEAMSTEERING EVALUATION

In order to comply with requirements for beamsteering with a transmitarray (360° phase control), 7 layer stacked unit cells have been considered to compose a 5×5 transmitarray. For this particular analysis, only the configuration of transmitarray defined by Case 1 will be considered for simulations, although the same study could be carried for Case 2. The final model o the transmitarray implemented in CST MWS is depicted in Fig. 4.5. The model was simulated using open boundaries and excited by an incident plane wave normal to the structure. The overall dimensions of the transmitarray are 28.75 x 28.75 x 7.87 mm^3 ($2.6\lambda_o$ x $2.6\lambda_o$ x $0.72\lambda_o$ at 28 GHz) and lumped elements were used to simulate the discrete capacitors.

In order to obtain the capacitance values required to place in each unit-cell, for a desired steering angle, a script was developed in Matlab environment. In a first instance, the script uses the formulation of Section 3.3 to compute the phase pattern to apply to the transmitarray for a specific angle. It receives as input the Azimuth and Elevation angle directions (in degrees) and it outputs a phase matrix with the dimensions of the array, as indicated in the matrix (3.6). Finally, the capacitance values are obtained by interpolating (using linear interpolation) the phase matrix with the theoretical phase curve for depicted in Fig. 4.2a, for 7 layers.

For demonstration, two different cases were considered: one for beamsteering in the azimuthal plane (Case A), and the other with beamsteering in both the azimuthal and elevation planes (Case B). In (4.2) and (4.3) the capacitance matrices obtained for both cases previously defined, are presented. For Case A, it was considered an azimuth of 16° and for Case B an azimuth and elevation of -18° and 13° were used, respectively. Note that the top left corner of the matrix refers to the capacitance value needed in the unit-cell of the top left corner when looking at the front of the transmitarray.

$$C_{x,y}= \begin{bmatrix} 0.48 & 0.58 & 0.76 & 1.24 & 2.80 \\ 0.48 & 0.58 & 0.76 & 1.24 & 2.80 \\ 0.48 & 0.58 & 0.76 & 1.24 & 2.80 \\ 0.48 & 0.58 & 0.76 & 1.24 & 2.80 \\ 0.48 & 0.58 & 0.76 & 1.24 & 2.80 \end{bmatrix} (pF) \tag{4.2}$$

$$C_{x,y}= \begin{bmatrix} 2.80 & 1.16 & 0.72 & 0.55 & 0.44 \\ 1.39 & 0.78 & 0.58 & 0.47 & 0.38 \\ 0.87 & 0.61 & 0.50 & 0.39 & 0.35 \\ 0.67 & 0.52 & 0.42 & 0.36 & 0.32 \\ 0.55 & 0.45 & 0.37 & 0.33 & 1.32 \end{bmatrix} (pF) \tag{4.3}$$

By loading the values of capacitance obtained to the lumped elements in the CST simulation environment, it can be observed that the transmitarray is capable of steering the main antenna beam towards the intended directions. This can observed by the Three-Dimensional (3D) radiation patterns of Fig. 4.6. In fact, a steering towards (Az,El) = (16°,0°) and (-18°,13°) is achieved with the 5×5 transmitarray, validating therefore the proposed beamsteering method.

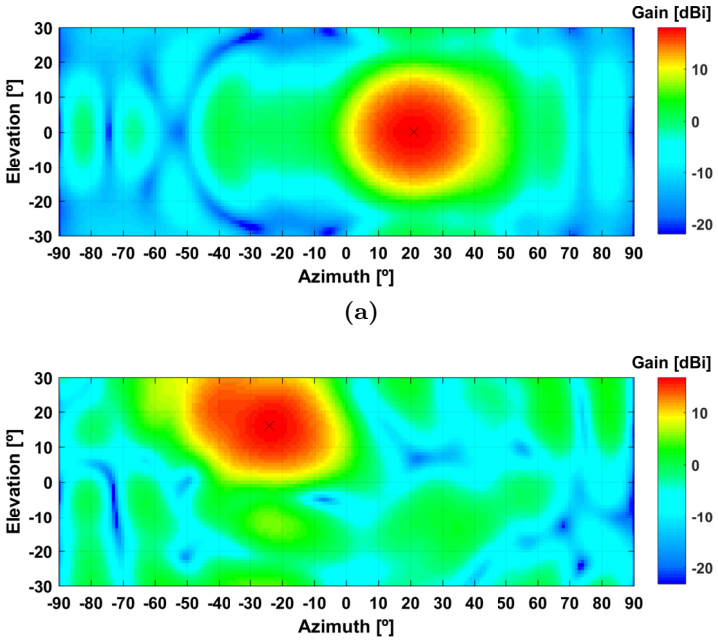

Figure 4.6: Simulated 3D radiation patterns considering (Az,El): (a) (16°,0°) and (b) (-18°,13°).

However, after an extended set of simulations including various output angle directions (Cases A to E), detailed in Table 4.5, a maximum angular deviation, consistently below 6°, is noticed. This deviation arise the need of an angular compensating model, being presented next section.

Table 4.5: Simulated beamsteering output angles

	Expected		Simulated		Error	
	Az (°)	El (°)	Az (°)	El (°)	Az (°)	El (°)
Case A	16	0	21	0	5	0
Case B	-18	13	-24	16	6	3
Case C	-20	20	-20	24	0	4
Case D	5	-8	7	-13	2	5
Case E	-18	-14	-24	-18	6	4
Average	-	-	-	-	3.8	3.2

4.4 OUTPUT ANGLE COMPENSATION

In order to mitigate the angle deviation previously observed, *i.e.* to compensate for the output steering angle deviation, a phase matching model has been studied. To this extent, a parametric study was carried out in order to model the angle deviation within the ±28°, as depicted Fig. 4.7, for both main radiation planes of the transmitarray, and summarized in Table 4.6. The phase matching model was evaluated from linear regression using (4.4) and (4.5), for both azimuth and elevation angles dependency, where S_{Az} and S_{El} are the simulated output angles for azimuth and elevation, respectively and E_{Az} and E_{El} are the expected (theoretical) output angles. Results presented in Fig. 4.7 show the relatively good agreement (fit) between the simulation results and the proposed model.

$$S_{Az}=1.4012 \times E_{Az} - 0.0179 \tag{4.4}$$

$$S_{El}=1.3254 \times E_{El} + 0.1305 \tag{4.5}$$

In order to assess the phase matching model effectiveness, the simulations presented in Table 4.5 were repeated, this time taking into account the compensation

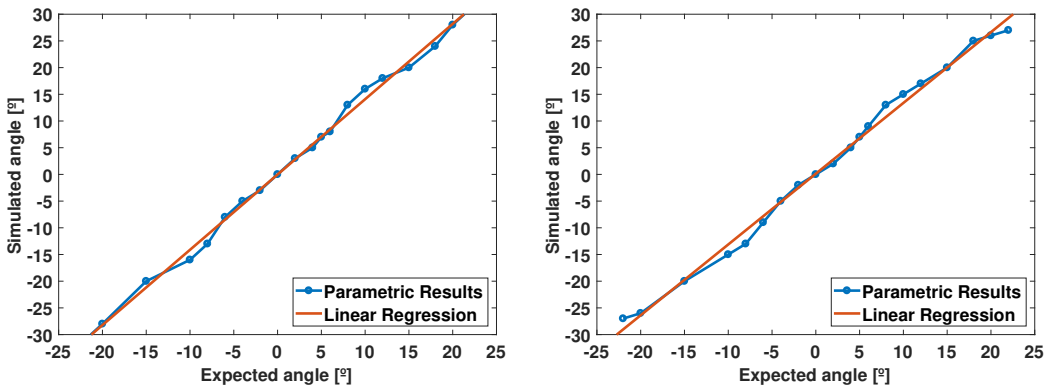

Figure 4.7: Phase matching model best fit for both (a) azimuth and (b) elevation planes.

Table 4.6: Expected vs simulated beamsteering angles.

Expected (°)	Azimuth (°)	Elevation (°)
-22	-31	-27
-20	-28	-26
-15	-20	-20
-10	-16	-15
-8	-13	-13
-6	-8	-9
-4	-5	-5
-2	-3	-2
0	0	0
2	3	2
4	5	5
5	7	7
6	8	9
8	13	13
10	16	15
12	18	17
15	20	20
18	24	25
20	28	26
22	31	27

algorithm. These are summarised in Table 4.7, and the steering cases A and B are depicted in Fig. 4.8, for comparison, against the ones originally presented in Fig. 4.6. The results clearly demonstrate that the proposed matching model is capable of correcting the beamsteering angle deviation while maintaining the original antenna radiation pattern integrity, with errors better than 1°.

The analysis present herein clearly proves the concept of antenna beamsteering using transmitarray at 28 GHz.

Table 4.7: Beamsteering results for phase compensation.

	Expected		Simulated			
			w/o compensation		w/ compensation	
	Az (°)	El (°)	Az (°)	El (°)	Az (°)	El (°)
Case A	16	0	21	0	17	0
Case B	-18	13	-24	16	-18	13
Case C	-20	20	-20	24	-19	-19
Case D	5	-8	7	-13	5	-8
Case E	-18	-14	-24	-18	-18	-13

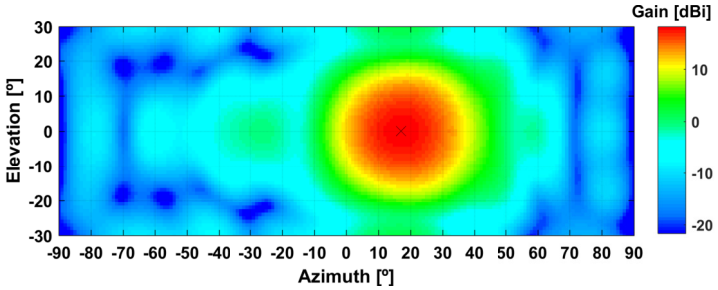

(a)

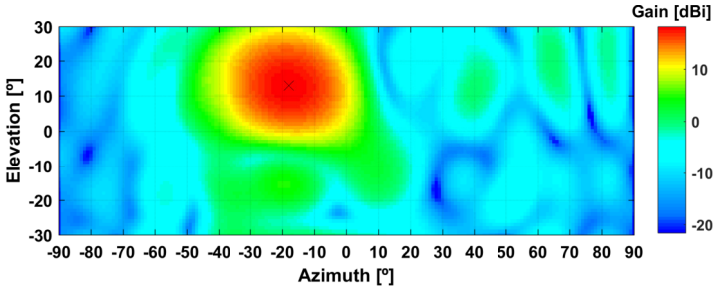

(b)

Figure 4.8: Optimised simulated 3D radiation patterns considering (Az,El): (a) (16°,0°) and (b) (-18°,13°).

4.5 INTERIM CONCLUSIONS

In this chapter the initial results and effectiveness of a transmitarray model with 2D antenna beamsteering capabilities, designed to operate at 28 GHz are presented. Simulation results indicate ±28° of beamsteering angle control, using a 5x5x7 stacked layer. The extension of the operating frequency to millimetre wave (mmWave) frequencies represented a leap reduction of the overall transmitarray dimensions by a factor of 6 and a fractional bandwidth of circa 2 %, yielding 500 MHz of physical bandwidth that makes it a good candidate for 5G and RADAR of the future applications. The idea of performing 2D beamsteering directly from standard high gain antenna using a single RF front-end is breakthrough in smart antenna design.

7

CONCLUSIONS

7.1 INTRODUCTION

In this chapter, conclusions of the developed work are drawn. A summary of the dissertation, as well as the main contributions to science resulting from this research and proposals for further work are presented herein. This chapter is divided in three more sections: a dissertation review by chapter; overview of the major contributions and lastly proposals for future development of the work presented in this dissertation.

7.2 DISSERTATION REVIEW

The main scope of this dissertation aimed at the investigation and implementation of a transmitarray to work at 28 GHz for 5G and RADAR applications. To achieve this main objective, a literature review on transmitarrays and antenna beamsteering technique was carried. A transmitarray inspired on FSS unit-cells have been designed, simulated, optimized and implemented. One prototype consisting of four transmitarrays has been characterized experimentally as a proof of concept to validate the usefulness of the methodology for antenna beamsteering at 28 GHz. Finally, the impact of the use of varactor diodes was studied in simulation environment to ascertain the feasibility of an electronically controlled transmitarray at such frequencies. A new cell design that takes these effects into account was also presented and fully characterized.

In Chapter 1 the background study and motivation of the work presented in this thesis were provided. This chapter then enumerated the main objectives and document structure.

Chapter 2 provided an extensive literature review on the existing transmitarray used both for beamsteering and polarisation control. Transmitarray unit-cells based on microstrip patches, FSS and MM and controlled by different means such as varactor or p-i-n diodes, among others, were analysed. All the transmitarrays were then summarised and their characteristics (such as size, frequency of operation, bandwidth and beamsteering range) compared to each other.

In Chapter 3 the mathematical concepts and formulas to perform beamsteering using a transmitarray were introduced.

The contents of Chapter 4 are related to the designing/re-dimensioning and optimisation of the FSS-based unit-cell, as well as it's capabilities when integrated in a full transmitarray. This was achieved through a complete parametric study based on EM simulations using CST MWS, which allowed to evaluate and characterise the transmitarray performance against unit-cell design parameters. Following the requirements of the theoretical model, a controlled phase shift is applied to each transmitarray element to enable 2D beamsteering. A fit model was also presented in order to correct the small errors in the beamsteering direction.

Chapter 5 presented the prototyping phase of four passive transmitarrays, as well as the measurements setups, results and post-processing analysis. Further simulations that were done during prototyping were still presented in this chapter (such as the effect of the discrete capacitor values and their respective tolerances) to ascertain how these factors impacted the overall performance of the structures. The prototypes were then implemented and their beamsteering characteristics studied in a controlled environment.

In Chapter 6 the first steps towards a 28 GHz electronically reconfigurable transmitarray based on a square-slot FSS were taken. In this chapter the effects of using a varactor diode, namely the parasitic inductance and resistance, were studied in simulation environment and compared to the ones considering a capacitor's ideal model. Having these results proven that the impact of the parasitics would make it impossible to perform beamsteering with this unit-cell, a new one was presented. The dual-polarisation characteristics of this new unit-cell were also studied in CST MWS.

7.3 CONTRIBUTIONS TO THE KNOWLEDGE

The research work carried out in this dissertation has contributed to the knowledge with relevant scientific publications in an international journal and several international conferences, covering most of the work presented throughout the different chapters of this dissertation.

At the time of submission of this document, the work being presented in this dissertation contributed to the knowledge with one journal paper and six conference papers (one of which has been accepted for presentation but not yet presented).

Papers in international journals

- J. R. Reis, M. Vala, R. F. S. Caldeirinha, **"Review paper on Transmitarray Antennas"**, *IEEE Access*, Vol. 7, No. 1, pp. 94171 - 94188, December, 2019.

Papers in conferences

- M. Vala, J. R. Reis, R. F. S. Caldeirinha, **"A Novel Dual-Polarised Transmitarray for Beamsteering at 28 GHz"**, *Antennas and Propagation Conference - APC*, Birmingham, United Kingdom, November, 2019 **(accepted for oral presentation)**;
- M. Vala, J. R. Reis, R. F. S. Caldeirinha, **"On the Practical Limitations of Electronic Beamsteering using Metamaterials at 28 GHz"**, *IEEE IEEE-APS Topical Conference on Antennas and Propagation in Wireless Communications APWC2019*, Granada, Spain, September, 2019;
- J. R. Reis, M. Vala, R. F. S. Caldeirinha, **"Novel Electronically Reconfigurable Transmitarray for 2D Beamsteering: Emerging Applications"**, *Conf. on Telecommunications - ConfTele*, Lisbon, Portugal, June, 2019;
- M. Vala, J. R. Reis, R. F. S. Caldeirinha, **"A 28 GHz Fully 2D Electronic Beamsteering Transmitarray for 5G and future RADAR applications"**, *Loughborough Antennas and Propagation Conf. – LAPC*, Loughborough, United Kingdom, November, 2018;
- M. Vala, A. Sardo, J. R. Reis, R. F. S. Caldeirinha, **"Electronic Reconfigurable Beam-redirecting Metasurfaces for Outdoor-indoor Radio Coverage Enhancement at 5.2 GHz"**, *IEEE International Symp. on Personal, Indoor and Mobile Radio Commun - PIMRC*, Bologne, Italy, September, 2018;
- R. F. S. Caldeirinha, J. R. Reis, M. Vala, A. Sardo, A. Hammoudeh, Nigel Copner, **"Electronically Reconfigurable Active Metamaterials for 2D Beamsteering"**, *Encuentro Ibérico de Electromagnetismo Computacional - EIEC*, Coimbra, Portugal, May, 2018.

7.4 FUTURE WORK

With the results obtained and presented in this dissertation, possible extension for further development may be suggested.

Future work will address further measurements and result verification on the implemented prototypes. Also, the fabrication of new prototypes without solder mask can be useful to understand how this parameter can influence the overall performance of the transmitarrays, when comparing to the prototypes already developed. This is sought to be a factor that will lead to better prototypes working in the intended frequency of operation. Besides, with new prototypes, it will also be possible to have more data on the influence of capacitor's tolerance by comparing prototypes steering the beam towards the same direction.

Furthermore, study on the new unit-cell intended be used on a fully electronically reconfigurable transmitarray using varactor diodes presented in Chapter 6 is also needed, namely in terms of the feeding network of the varactors. Besides, even though a study of the varactor diodes present in the market was carried, the advancement of technology may allow for new varactor diodes that could lead to better results in this new unit-cell.

Consideration should be given to conformal solutions that would allow complete 360° field of view, in which several transmitarrays may be used in a sectoral configuration.

BIBLIOGRAPHY

[1] C. A. Balanis, *Antenna Theory: Analysis and Design, 3rd Edition*. John Wiley & Sons, 2005, vol. 72.

[2] R. J. Mailloux, *Phased Array Antenna Handbook*. Artech House, Incorporated, 2005.

[3] A. Bhattacharyya, *Phased Array Antennas: Floquet Analysis, Synthesis, Bfns and Active Array Systems*, ser. Wiley Series in Microwave and Optical Engineering. Wiley, 2006.

[4] J. Lee, E. Tejedor, K. Ranta-aho, H. Wang, K.-T. Lee, E. Semaan, E. Mohyeldin, J. Song, C. Bergljung, and S. Jung, "Spectrum for 5g: Global status, challenges, and enabling technologies," *IEEE Communications Magazine*, vol. 56, no. 3, pp. 12–18, mar 2018.

[5] J. R. Reis, "Novel antenna beamsteering for wireless applications," Ph.D. dissertation, University of South Wales, 2018.

[6] F. Capolino, *Applications of Metamaterials*. CRC Press, 2009.

[7] C. Balanis, *Advanced Engineering Electromagnetics*, ser. CourseSmart Series. Wiley, 2012.

[8] J. Vardaxoglou, *Frequency Selective Surfaces: Analysis and Design*. Research Studies Press, 1997.

[9] B. A. Munk, *Frequency Selective Surfaces: Theory and Design*. John Wiley & Sons, 2005.

[10] K. Sarabandi and N. Behdad, "A Frequency Selective Surface With Miniaturized Elements," *IEEE Transactions on Antennas and Propagation*, vol. 55, no. 5, pp. 1239–1245, May 2007.

[11] D. Ferreira, R. Caldeirinha, I. Cuiñas, and T. Fernandes, "Square Loop and Slot Frequency Selective Surfaces Study for Equivalent Circuit Model Optimization," *IEEE Transactions on Antennas and Propagation*, vol. 63, no. 9, pp. 3947–3955, Sept 2015.

[12] D. McGrath, "Planar Three-Dimensional Constrained Lenses," *IEEE Transactions on Antennas and Propagation*, vol. 34, no. 1, pp. 46–50, Jan 1986.

[13] J. Y. Lau, "Reconfigurable Transmitarray Antennas," Ph.D. dissertation, University of Toronto, 2012.

[14] L. D. Palma, "Reconfigurable Transmitarray Antennas at Millimeter-Wave Frequencies," Ph.D., 2015.

[15] S. Hum and J. Perruisseau-Carrier, "Reconfigurable Reflectarrays and Array Lenses for Dynamic Antenna Beam Control: A Review," *IEEE Transactions on Antennas and Propagation*, vol. 62, no. 1, pp. 183–198, Jan 2014.

[16] M. Maasch, M. Roig, C. Damm, and R. Jakoby, "Voltage-tunable artificial gradient-index lens based on a liquid crystal loaded fishnet metamaterial," *IEEE Antennas and Wireless Propagation Letters*, vol. 13, pp. 1581–1584, 2014.

[17] Y. Huang, L. Wu, M. Tang, and J. Mao, "Design of a Beam Reconfigurable THz Antenna With Graphene-Based Switchable High-Impedance Surface," *IEEE Transactions on Nanotechnology*, vol. 11, no. 4, pp. 836–842, July 2012.

[18] E. Carrasco, M. Tamagnone, and J. Perruisseau-Carrier, "Tunable Graphene-based Reflectarray Element for Reconfigurable Beams," in *2013 7th European Conference on Antennas and Propagation (EuCAP)*, April 2013, pp. 1779–1782.

[19] H. A. Malhat, S. H. Zainud-Deen, and S. M. Gaber, "Circularly Polarized Graphene Based Transmitarray for Terahertz Applications," in *2014 XXXIth URSI General Assembly and Scientific Symposium (URSI GASS)*, Aug 2014, pp. 1–4.

[20] W. M. Hassan, S. H. Zainud-Deen, and H. A. Malhat, "Compact Multi-function Single/dual-beam Graphene Lens Antenna for Terahertz Applications," in *2016 33rd National Radio Science Conference (NRSC)*, Feb 2016, pp. 41–48.

[21] W. M. Hassan, "Multilayer Graphene-only Transmitarray Antenna (MGOT) for Terahertz Applications," in *2017 34th National Radio Science Conference (NRSC)*, March 2017, pp. 43–48.

[22] W. Yao, L. Tang, J. Wang, C. Ji, X. Wei, and Y. Jiang, "Spectrally and Spatially Tunable Terahertz Metasurface Lens Based on Graphene Surface Plasmons," *IEEE Photonics Journal*, vol. 10, no. 4, pp. 1–8, Aug 2018.

[23] A. Moessinger, R. Marin, S. Mueller, J. Freese, and R. Jakoby, "Electronically reconfigurable reflectarrays with nematic liquid crystals," *Electronics Letters*, vol. 42, no. 16, pp. 899–900, August 2006.

[24] G. Perez-Palomino, J. A. Encinar, M. Barba, and E. Carrasco, "Design and Evaluation of Multi-resonant Unit Cells Based on Liquid Crystals for Reconfigurable Reflectarrays," *IET Microwaves, Antennas Propagation*, vol. 6, no. 3, pp. 348–354, February 2012.

[25] S. Bildik, S. Dieter, C. Fritzsch, W. Menzel, and R. Jakoby, "Reconfigurable Folded Reflectarray Antenna Based Upon Liquid Crystal Technology," *IEEE Transactions on Antennas and Propagation*, vol. 63, no. 1, pp. 122–132, Jan

2015.

[26] G. Perez-Palomino, M. Barba, J. A. Encinar, R. Cahill, R. Dickie, P. Baine, and M. Bain, "Design and demonstration of an electronically scanned reflectarray antenna at 100 ghz using multiresonant cells based on liquid crystals," *IEEE Transactions on Antennas and Propagation*, vol. 63, no. 8, pp. 3722–3727, Aug 2015.

[27] Y. Zhao, C. Huang, A. Qing, and X. Luo, "A Frequency and Pattern Reconfigurable Antenna Array Based on Liquid Crystal Technology," *IEEE Photonics Journal*, vol. 9, no. 3, pp. 1–7, June 2017.

[28] B. Che, T. Jin, D. Erni, F. Meng, Y. Lyu, and Q. Wu, "Electrically controllable composite right/left-handed leaky-wave antenna using liquid crystals in pcb technology," *IEEE Transactions on Components, Packaging and Manufacturing Technology*, vol. 7, no. 8, pp. 1331–1342, Aug 2017.

[29] S. F. Jilani, M. O. Munoz, Q. H. Abbasi, and A. Alomainy, "Millimeter-Wave Liquid Crystal Polymer Based Conformal Antenna Array for 5G Applications," *IEEE Antennas and Wireless Propagation Letters*, vol. 18, no. 1, pp. 84–88, Jan 2019.

[30] S. H. Lee, M. Choi, T.-T. Kim, S. Lee, M. Liu, X. Yin, H. K. Choi, S. S. Lee, C.-G. Choi, S.-Y. Choi, X. Zhang, and B. Min, "Switching terahertz waves with gate-controlled active graphene metamaterials," *Nature Materials*, vol. 11, pp. 936 EP –, Sep 2012. [Online]. Available: https://doi.org/10.1038/nmat3433

[31] C. Núñez Álvarez, R. Cheung, and J. S. Thompson, "Performance Analysis of Hybrid Metal–Graphene Frequency Reconfigurable Antennas in the Microwave Regime," *IEEE Transactions on Antennas and Propagation*, vol. 65, no. 4, pp. 1558–1569, April 2017.

[32] J. Shaker, M. R. Chaharmir, and J. Ethier, *Reflectarray Antennas: Analysis, Design, Fabrication, and Measurement*. Artech House, 2013, vol. 1.

[33] J. Huang and J. A. Encinar, *Reflectarray Antennas*. John Wiley & Sons, 2007, vol. 9.

[34] D. M. Pozar, S. D. Targonski, and H. Syrigos, "Design of Millimeter Wave Microstrip Reflectarrays," *IEEE Transactions on Antennas and Propagation*, vol. 45, no. 2, pp. 287–296, Feb 1997.

[35] D. Sievenpiper, J. Schaffner, R. Loo, G. Tangonan, S. Ontiveros, and R. Harold, "A Tunable Impedance Surface Performing as a Reconfigurable Beam Steering Reflector," *IEEE Transactions on Antennas and Propagation*, vol. 50, no. 3, pp. 384–390, Mar 2002.

[36] D. Sievenpiper and J. Schaffner, "Beam Steering Microwave Reflector Based on Electrically Tunable Impedance Surface," *Electronics Letters*, vol. 38, no. 21, pp. 1237–1238, Oct 2002.

[37] E. Carrasco, M. Barba, B. Reig, C. Dieppedale, and J. Encinar, "Characterization of a Reflectarray Gathered Element With Electronic Control Using Ohmic RF MEMS and Patches Aperture-Coupled to a Delay Line," *IEEE Transactions on Antennas and Propagation*, vol. 60, no. 9, pp. 4190–4201, Sept 2012.

[38] E. Carrasco, M. Barba, and J. Encinar, "X-Band Reflectarray Antenna With Switching-Beam Using PIN Diodes and Gathered Elements," *IEEE Transactions on Antennas and Propagation*, vol. 60, no. 12, pp. 5700–5708, Dec 2012.

[39] P. Padilla, A. Munoz-Acevedo, M. Sierra-Castaner, and M. Sierra-Perez, "Electronically Reconfigurable Transmitarray at Ku Band for Microwave Applications," *IEEE Transactions on Antennas and Propagation*, vol. 58, no. 8, pp. 2571–2579, Aug 2010.

[40] J. Y. Lau and S. V. Hum, "Analysis and Characterization of a Multipole Reconfigurable Transmitarray Element," *IEEE Transactions on Antennas and Propagation*, vol. 59, no. 1, pp. 70–79, Jan 2011.

[41] J. Lau and S. Hum, "A Planar Reconfigurable Aperture With Lens and Reflectarray Modes of Operation," *IEEE Transactions on Microwave Theory and Techniques*, vol. 58, no. 12, pp. 3547–3555, Dec 2010.

[42] ——, "A Wideband Reconfigurable Transmitarray Element," *IEEE Transactions on Antennas and Propagation*, vol. 60, no. 3, pp. 1303–1311, March 2012.

[43] ——, "Reconfigurable Transmitarray Design Approaches for Beamforming Applications," *IEEE Transactions on Antennas and Propagation*, vol. 60, no. 12, pp. 5679–5689, Dec 2012.

[44] A. Clemente, L. Dussopt, R. Sauleau, P. Potier, and P. Pouliguen, "1-bit Reconfigurable Unit Cell Based on PIN Diodes for Transmit-array Applications in X-band," *IEEE Transactions on Antennas and Propagation*, vol. 60, no. 5, pp. 2260–2269, May 2012.

[45] A. Clemente, L. Dussopt, B. Reig, R. Sauleau, P. Potier, and P. Pouliguen, "Reconfigurable Unit-cells for Beam-scanning Transmitarrays in X Band," in *2013 7th European Conference on Antennas and Propagation (EuCAP)*, April 2013, pp. 1783–1787.

[46] A. Clemente, L. Dussopt, R. Sauleau, P. Potier, and P. Pouliguen, "Wideband 400-Element Electronically Reconfigurable Transmitarray in X Band," *IEEE Transactions on Antennas and Propagation*, vol. 61, no. 10, pp. 5017–5027, Oct 2013.

[47] F. Diaby, A. Clemente, L. D. Palma, L. Dussopt, K. Pham, E. Fourn, and R. Sauleau, "Design of a 2-bit unit-cell for electronically reconfigurable transmitarrays at ka-band," in *2017 47th European Microwave Conference (EuMC)*. IEEE, oct 2017.

[48] M. Frank, F. Lurz, R. Weigel, and A. Koelpin, "Electronically reconfigurable 6 × 6 element transmitarray at k band based on unit-cells with continuous phase range," *IEEE Antennas and Wireless Propagation Letters*, pp. 1–1, 2019.

[49] Y. Sun, Z. Li, W. Zhu, Z. Ji, and Q. Wang, "New Steerable Antenna with Controllable Metamaterial," in *EuMC 2012 European Microwave Conference*, Oct 2012, pp. 936–939.

[50] T. Jiang, Z. Wang, D. Li, J. Pan, B. Zhang, J. Huangfu, Y. Salamin, C. Li, and L. Ran, "Low-DC Voltage-Controlled Steering-Antenna Radome Utilizing Tunable Active Metamaterial," *IEEE Transactions on Microwave Theory and Techniques*, vol. 60, no. 1, pp. 170–178, Jan. 2012.

[51] C. G. Ryan, M. Chaharmir, J. Shaker, J. Bray, Y. Antar, and A. Ittipiboon, "A Wideband Transmitarray Using Dual-Resonant Double Square Rings," *IEEE Transactions on Antennas and Propagation*, vol. 58, no. 5, pp. 1486–1493, May 2010.

[52] I. Russo, D. Gaetano, L. Boccia, G. Amendola, and G. Di Massa, "Investigation on the Transmission Beam-Steering Capabilities of Tunable Impedance Surfaces," in *EuMC 2009 European Microwave Conference*, Sept 2009, pp. 1033–1036.

[53] I. Russo, L. Boccia, G. Amendola, and G. Di Massa, "Tunable Pass-band FSS for Beam Steering Applications," in *2010 Proceedings of the Fourth European Conference on Antennas and Propagation (EuCAP)*, April 2010, pp. 1–4.

[54] L. Boccia, I. Russo, G. Amendola, and G. Di Massa, "Multilayer Antenna-Filter Antenna for Beam-Steering Transmit-Array Applications," *IEEE Transactions on Microwave Theory and Techniques*, vol. 60, no. 7, pp. 2287–2300, July 2012.

[55] W. Pan, C. Huang, P. Chen, M. Pu, X. Ma, and X. Luo, "A Beam Steering Horn Antenna Using Active Frequency Selective Surface," *IEEE Transactions on Antennas and Propagation*, vol. 61, no. 12, pp. 6218–6223, Dec 2013.

[56] M. Sazegar, Y. Zheng, C. Kohler, H. Maune, M. Nikfalazar, J. Binder, and R. Jakoby, "Beam Steering Transmitarray Using Tunable Frequency Selec-

tive Surface With Integrated Ferroelectric Varactors," *IEEE Transactions on Antennas and Propagation*, vol. 60, no. 12, pp. 5690–5699, Dec 2012.

[57] J. R. Reis, N. Copner, A. Hammoudeh, Z. M. E. Al-Daher, R. F. S. Caldeirinha, T. R. Fernandes, and R. Gomes, "FSS-Inspired Transmitarray for Two-Dimensional Antenna Beamsteering," *IEEE Transactions on Antennas and Propagation*, vol. 64, no. 6, pp. 2197–2206, June 2016.

[58] J. R. Reis, R. F. S. Caldeirinha, A. Hammoudeh, and N. Copner, "Electronically Reconfigurable FSS-Inspired Transmitarray for 2-D Beamsteering," *IEEE Transactions on Antennas and Propagation*, vol. 65, no. 9, pp. 4880–4885, Sept 2017.

[59] B. D. Nguyen and C. Pichot, "Unit-cell loaded with PIN diodes for 1-bit linearly polarized reconfigurable transmitarrays," *IEEE Antennas and Wireless Propagation Letters*, vol. 18, no. 1, pp. 98–102, jan 2019.

[60] A. Edalati and T. Denidni, "Beam-switching Antenna Based on Active Frequency Selective Surfaces," in *2011 IEEE International Symposium on Antennas and Propagation (APSURSI)*, July 2011, pp. 2254–2257.

[61] H. Zhou, S. Qu, B. Lin, J. Wang, H. Ma, Z. Xu, W. Peng, and P. Bai, "Filter-Antenna Consisting of Conical FSS Radome and Monopole Antenna," *IEEE Transactions on Antennas and Propagation*, vol. 60, no. 6, pp. 3040–3045, June 2012.

[62] M. Niroo-Jazi and T. Denidni, "Electronically Sweeping-Beam Antenna Using a New Cylindrical Frequency-Selective Surface," *IEEE Transactions on Antennas and Propagation*, vol. 61, no. 2, pp. 666–676, Feb 2013.

[63] M. Vala, A. Sardo, J. R. Reis, and R. F. S. Caldeirinha, "Electronic reconfigurable beam-redirecting metasurfaces for outdoor-indoor radio coverage enhancement at 5.2 GHz," in *2018 IEEE 29th Annual International Symposium on Personal, Indoor and Mobile Radio Communications (PIMRC)*. IEEE, sep 2018.

[64] H. Kaouach, L. Dussopt, J. Lanteri, T. Koleck, and R. Sauleau, "Circularly-polarized Discrete Lens Antennas in the 60-GHz Band," in *2010 Conference Proceedings ICECom*, Sept 2010, pp. 1–4.

[65] L. Dussopt, H. Kaouach, J. Lanteri, and R. Sauleau, "Circularly-polarized Discrete Lens Antennas in the 60-GHz Band," in *Radio Engineering*, vol. 20, Dec 2011, pp. 733–738.

[66] L. D. Palma, A. Clemente, L. Dussopt, R. Sauleau, P. Potier, and P. Pouliguen, "Circularly Polarized Transmitarray With Sequential Rotation in Ka-Band," *IEEE Transactions on Antennas and Propagation*, vol. 63, no. 11, pp. 5118–5124,

Nov 2015.

[67] C. Pfeiffer and A. Grbic, "Millimeter-Wave Transmitarrays for Wavefront and Polarization Control," *IEEE Transactions on Microwave Theory and Techniques*, vol. 61, no. 12, pp. 4407–4417, Dec 2013.

[68] X. Zhong, L. Chen, Y. Shi, and X. Shi, "Design of Multiple-Polarization Transmitarray Antenna Using Rectangle Ring Slot Elements," *IEEE Antennas and Wireless Propagation Letters*, vol. 15, pp. 1803–1806, 2016.

[69] P. Naseri, S. A. Matos, J. R. Costa, and C. A. Fernandes, "Phase-Delay Versus Phase-Rotation Cells for Circular Polarization Transmit Arrays - Application to Satellite Ka-Band Beam Steering," *IEEE Transactions on Antennas and Propagation*, vol. 66, no. 3, pp. 1236–1247, March 2018.

[70] S. Hollung, A. E. Cox, and Z. B. Popovic, "A Bi-directional Quasi-optical Lens Amplifier," *IEEE Transactions on Microwave Theory and Techniques*, vol. 45, no. 12, pp. 2352–2357, Dec 1997.

[71] E. W. Bryerton, M. D. Weiss, and Z. Popovic, "A 10-GHz High-efficiency Lens Amplifier Array," in *1998 IEEE MTT-S International Microwave Symposium Digest (Cat. No.98CH36192)*, vol. 3, June 1998, pp. 1461–1464 vol.3.

[72] S. C. Ortiz, T. Ivanov, and A. Mortazawi, "A Cpw-fed Microstrip Patch Quasi-optical Amplifier Array," *IEEE Transactions on Microwave Theory and Techniques*, vol. 48, no. 2, pp. 276–280, Feb 2000.

[73] H. J. Song and M. E. Bialkowski, "Transmit Array of Transistor Amplifiers Illuminated by a Patch Array in the Reactive Near-field Region," *IEEE Transactions on Microwave Theory and Techniques*, vol. 49, no. 3, pp. 470–475, March 2001.

[74] S. C. Ortiz, J. Hubert, L. Mirth, E. Schlecht, and A. Mortazawi, "A High-power Ka-band Quasi-optical Amplifier Array," *IEEE Transactions on Microwave Theory and Techniques*, vol. 50, no. 2, pp. 487–494, Feb 2002.

[75] W. Pan, C. Huang, X. Ma, and X. Luo, "An amplifying tunable transmitarray element," *IEEE Antennas and Wireless Propagation Letters*, vol. 13, pp. 702–705, 2014.

[76] N. Landsberg and E. Socher, "Multi-level Ask Spatial Modulators Employing a 100 GHz Lens-array Antenna and 65 nm CMOS," in *2016 46th European Microwave Conference (EuMC)*, Oct 2016, pp. 429–432.

[77] ——, "Design and Measurements of 100 GHz Reflectarray and Transmitarray Active Antenna Cells," *IEEE Transactions on Antennas and Propagation*, vol. 65, no. 12, pp. 6986–6997, Dec 2017.

[78] C. Huang, W. Pan, X. Ma, B. Zhao, J. Cui, and X. Luo, "Using Reconfigurable Transmitarray to Achieve Beam-Steering and Polarization Manipulation Applications," *IEEE Transactions on Antennas and Propagation*, vol. 63, no. 11, pp. 4801–4810, Nov 2015.

[79] C. Huang, W. Pan, X. Ma, and X. Luo, "1-Bit Reconfigurable Circularly Polarized Transmitarray in X-Band," *IEEE Antennas and Wireless Propagation Letters*, vol. 15, pp. 448–451, 2016.

[80] C. Huang, W. Pan, and X. Luo, "Low-Loss Circularly Polarized Transmitarray for Beam Steering Application," *IEEE Transactions on Antennas and Propagation*, vol. 64, no. 10, pp. 4471–4476, Oct 2016.

[81] L. D. Palma, A. Clemente, L. Dussopt, R. Sauleau, P. Potier, and P. Pouliguen, "Circularly-Polarized Reconfigurable Transmitarray in Ka-Band With Beam Scanning and Polarization Switching Capabilities," *IEEE Transactions on Antennas and Propagation*, vol. 65, no. 2, pp. 529–540, Feb 2017.

[82] M. Wang, S. Xu, F. Yang, and M. Li, "Design and measurement of a 1-bit reconfigurable transmitarray with sub-wavelength h-shaped coupling slot elements," *IEEE Transactions on Antennas and Propagation*, pp. 1–1, 2019.

[83] E. B. Lima, S. A. Matos, J. R. Costa, C. A. Fernandes, and N. J. G. Fonseca, "Circular polarization wide-angle beam steering at ka-band by in-plane translation of a plate lens antenna," *IEEE Transactions on Antennas and Propagation*, vol. 63, no. 12, pp. 5443–5455, Dec 2015.

[84] G. Masters and S. Gregson, "Coordinate System Plotting for Antenna Measurements," *AMTA Symposium*, 2007.

[85] D. Pozar, *Microwave Engineering*, 4th ed. John Wiley and Sons Ltd, 2012.

[86] FlannMicrowave. Dual Polarized Horn Series DP241. [Online]. Available: https://flann.com/wp-content/uploads/2015/09/Series-DP241.pdf

[87] SKYWORKS. Smv2019 to smv2023 series: Hyperabrupt junction tuning varactors. [Online]. Available: http://www.skyworksinc.com/uploads/documents/SMV2019_to_SMV2023_Series_200074Q.pdf

[88] ——. Smv2201-smv2205 series: Surface mount, 0402 silicon hyperabrupt tuning varactor diodes. [Online]. Available: http://www.skyworksinc.com/uploads/documents/201953A.pdf

[89] ——. Smv1405 to smv1430 series: Plastic packaged abrupt junction tuning varactors. [Online]. Available: http://www.skyworksinc.com/uploads/documents/SMV1405_1430_Series_200068V.pdf

[90] Microsemi. Mpv1965 & mpv2100. [Online]. Available: https://www.microsemi.com/document-portal/doc_view/9526-mpv1965-mpv2100-series-datasheet

DECLARATION

Declaro, sob compromisso de honra, que o trabalho apresentado nesta dissertação, com o título *"Electronically Reconfigurable FSS-Inspired Transmitarray for Two Dimensional Beamsteering for 5G and RADAR Applications at 28 GHz"*, é original e foi realizado por Mário António Patrício Carreira Vala (2172276) sob orientação de Professor Rafael F. S. Caldeirinha (rafael.caldeirinha@ipleiria.pt) e Doctor João R. Reis (joao.reis@ipleiria.pt).

Leiria, September of 2019

Mário António Patrício Carreira Vala